

Let’s Make Block Coordinate Descent Go Fast: Faster Greedy Rules, Message-Passing, Active-Set Complexity, and Superlinear Convergence

Julie Nutini*

Issam Laradji†

Mark Schmidt‡

February 5, 2018

Abstract

Block coordinate descent (BCD) methods are widely-used for large-scale numerical optimization because of their cheap iteration costs, low memory requirements, amenability to parallelization, and ability to exploit problem structure. Three main algorithmic choices influence the performance of BCD methods: the block partitioning strategy, the block selection rule, and the block update rule. In this paper we explore all three of these building blocks and propose variations for each that can lead to significantly faster BCD methods. We (i) propose new greedy block-selection strategies that guarantee more progress per iteration than the Gauss-Southwell rule; (ii) explore practical issues like how to implement the new rules when using “variable” blocks; (iii) explore the use of message-passing to compute matrix or Newton updates efficiently on huge blocks for problems with a sparse dependency between variables; and (iv) consider optimal active manifold identification, which leads to bounds on the “active-set complexity” of BCD methods and leads to superlinear convergence for certain problems with sparse solutions (and in some cases finite termination at an optimal solution). We support all of our findings with numerical results for the classic machine learning problems of least squares, logistic regression, multi-class logistic regression, label propagation, and L1-regularization.

1 Introduction

Block coordinate descent (BCD) methods have become one of our key tools for solving some of the most important large-scale optimization problems. This is due to their typical ease of implementation, low memory requirements, cheap iteration costs, adaptability to distributed settings, ability to use problem structure, and numerical performance. Notably, they have been used for almost two decades in the context of L1-regularized least squares (LASSO) [Fu, 1998, Sardy et al., 2000] and support vector machines (SVMs) [Chang and Lin, 2011, Joachims, 1999]. Indeed, randomized BCD methods have recently been used to solve instances of these widely-used models with a billion variables [Richtárik and Takáč, 2014], while for “kernelized” SVMs *greedy* BCD methods remain among the state of the art methods [You et al., 2016]. Due to the wide use of these models, any improvements on the convergence of BCD methods will affect a myriad of applications.

While there are a variety of ways to implement a BCD method, the three main building blocks that affect its performance are:

1. **Blocking strategy.** We need to define a set of possible “blocks” of problem variables that we might choose to update at a particular iteration. Two common strategies are to form a partition of the coordinates into disjoint sets (we call this *fixed* blocks) or to consider any possible subset of coordinates as a “block” (we call this *variable* blocks). Typical choices include using a set of fixed blocks related to the problem structure, or using variable blocks by randomly sampling a fixed number of coordinates.

*Department of Computer Science, University of British Columbia (jnutini@cs.ubc.ca).

†Department of Computer Science, University of British Columbia (issamou@cs.ubc.ca).

‡Department of Computer Science, University of British Columbia (schmidt@cs.ubc.ca).

2. **Block selection rule.** Given a set of possible blocks, we need a rule to select a block of corresponding variables to update. Classic choices include cyclically going through a fixed ordering of blocks, choosing random blocks, choosing the block with the largest gradient (the *Gauss-Southwell* rule), or choosing the block that leads to the largest improvement.
3. **Block update rule.** Given the block we have selected, we need to decide how to update the block of corresponding variables. Typical choices include performing a gradient descent iteration, computing the Newton direction and performing a line-search, or computing the optimal update of the block by subspace minimization.

In the next section we introduce our notation, review the standard choices behind BCD algorithms, and discuss problem structures where BCD is suitable. Subsequently, the following sections explore a wide variety of ways to speed up BCD by modifying the three building blocks above.

1. In Section 3 we propose block selection rules that are variants of the Gauss-Southwell rule, but that incorporate knowledge of Lipschitz constants in order to give better bounds on the progress made at each iteration. We also give a general result characterizing the convergence rate obtained using the Gauss-Southwell rule as well as the new greedy rules, under both the Polyak-Lojasiewicz inequality and for general (potentially non-convex) functions.
2. In Section 4 we discuss practical implementation issues. This includes how to approximate the new rules in the variable-block setting, how to estimate the Lipschitz constants, how to efficiently implement line-searches, how the blocking strategy interacts with greedy rules, and why we should prefer Newton updates over the “matrix updates” of recent works.
3. In Section 5 we show how second-order updates, or the exact update for quadratic functions, can be computed in linear-time for problems with sparse dependencies when using “forest-structured” blocks. This allows us to use huge block sizes for problems with sparse dependencies, and uses a connection between sparse quadratic functions and Gaussian Markov random fields (GMRFs) by exploiting the “message-passing” algorithms developed for GMRFs.
4. In Section 6 we show that greedy BCD methods have a finite-time manifold identification property for problems with separable non-smooth structures like bound constraints or L1-regularization. Our analysis notably leads to bounds on the number of iterations required to reach the optimal manifold (“active-set complexity”). Further, when using greedy rules with variable blocks this leads to super-linear convergence for problems with sufficiently-sparse solutions (when we use updates incorporating second-order information). In the special case of LASSO and SVM problems, we further show that optimal updates are possible. This leads to finite convergence for SVM and LASSO problems with sufficiently-sparse solutions when using greedy selection and sufficiently-large variable blocks.

We note that many related ideas have been explored by others in the context of BCD methods and we will go into detail about these related works in subsequent sections. In Section 7 we use a variety of problems arising in machine learning to evaluate the effects of these choices on BCD implementations. These experiments indicate that in some cases the performance improvement obtained by using these enhanced methods can be dramatic. The source code and data files required to reproduce the experimental results of this paper can be downloaded from: <https://github.com/IssamLaradji/BlockCoordinateDescent>.

2 Block Coordinate Descent Algorithms

We first consider the problem of minimizing a differentiable multivariate function,

$$\arg \min_{x \in \mathbb{R}^n} f(x). \tag{1}$$

At iteration k of a BCD algorithm, we first select a block $b_k \subseteq \{1, 2, \dots, n\}$ and then update the subvector $x_{b_k} \in \mathbb{R}^{|b_k|}$ corresponding to these variables,

$$x_{b_k}^{k+1} = x_{b_k}^k + d^k.$$

Coordinates of x^{k+1} that are not included in b_k are simply kept at their previous value. The vector $d^k \in \mathbb{R}^{|b_k|}$ is typically selected to provide descent in the direction of the reduced dimensional subproblem,

$$d^k \in \arg \min_{d \in \mathbb{R}^{|b_k|}} f(x^k + U_{b_k} d), \quad (2)$$

where we construct $U_{b_k} \in \{0, 1\}^{n \times |b_k|}$ from the columns of the identity matrix corresponding to the coordinates in b_k . Using this notation, we have

$$x_{b_k} = U_{b_k}^T x,$$

which allows us to write the BCD update of all n variables in the form

$$x^{k+1} = x^k + U_{b_k} d^k.$$

There are many possible ways to define the block b_k as well as the direction d^k . Typically we have a maximum block size τ , which is chosen to be the largest number of variables that we can efficiently update at once. Given τ that divides evenly into n , consider a simple ordered fixed partition of the coordinates into a set \mathcal{B} of n/τ blocks,

$$\mathcal{B} = \{\{1, 2, \dots, \tau\}, \{\tau + 1, \tau + 2, \dots, 2\tau\}, \dots, \{(n - \tau) + 1, (n - \tau) + 2, \dots, n\}\}.$$

To select the block in \mathcal{B} to update at each iteration we could simply repeatedly cycle through this set in order. A simple choice of d^k is the negative gradient corresponding to the coordinates in b_k , multiplied by a scalar step-size α_k that is sufficiently small to ensure that we decrease the objective function. This leads to a gradient update of the form

$$x^{k+1} = x^k - \alpha_k U_{b_k} \nabla_{b_k} f(x^k), \quad (3)$$

where $\nabla_{b_k} f(x^k)$ are the elements of the gradient $\nabla f(x^k)$ corresponding to the coordinates in b_k . While this gradient update and cyclic selection among an ordered fixed partition is simple, we can often drastically improve the performance using more clever choices. We highlight some common alternative choices in the next three subsections.

2.1 Block Selection Rules

Repeatedly going through a fixed partition of the coordinates is known as *cyclic* selection [Bertsekas, 2016], and this is referred to as Gauss-Seidel when solving linear systems [Ortega and Rheinboldt, 1970]. The performance of cyclic selection may suffer if the order the blocks are cycled through is chosen poorly, but it has been shown that random permutations can fix a worst case for cyclic CD [Lee and Wright, 2016]. A variation on cyclic selection is “essentially” cyclic selection where each block must be selected at least every m iterations for some fixed m that is larger than the number of blocks [Bertsekas, 2016]. Alternately, several authors have explored the advantages of *randomized* block selection [Nesterov, 2010, Richtárik and Takáč, 2014]. The simplest randomized selection rule is to select one of the blocks uniformly at random. However, several recent works show dramatic performance improvements over this naive random sampling by incorporating knowledge of the Lipschitz continuity properties of the gradients of the blocks [Nesterov, 2010, Qu and Richtárik, 2016, Richtárik and Takáč, 2016] or more recently by trying to estimate the optimal sampling distribution online [Namkoong et al., 2017].

An alternative to cyclic and random block selection is *greedy* selection. Greedy methods solve an optimization problem to select the “best” block at each iteration. A classic example of greedy selection is the **block Gauss-Southwell** (GS) rule, which chooses the block whose gradient has the largest Euclidean norm,

$$b_k \in \arg \max_{b \in \mathcal{B}} \|\nabla_b f(x^k)\|, \quad (4)$$

where we use \mathcal{B} as the set of possible blocks. This rule tends to make more progress per iteration in theory and practice than randomized selection [Dhillon et al., 2011, Nutini et al., 2015]. Unfortunately, for many problems it is more expensive than cyclic or randomized selection. However, several recent works show that certain problem structures allow efficient calculation of GS-style rules [Fountoulakis et al., 2016, Lei et al., 2016, Meshi et al., 2012, Nutini et al., 2015], allow efficient approximation of GS-style rules [Dhillon et al., 2011, Stich et al., 2017, Thoppe et al., 2014], or allow other rules that try to improve on the progress made at each iteration [Csiba et al., 2015, Glasmachers and Dogan, 2013].

The ideal selection rule is the maximum improvement (MI) rule, which chooses the block that decreases the function value by the largest amount. Notable recent applications of this rule include leading eigenvector computation [Li et al., 2015], polynomial optimization [Chen et al., 2012], and fitting Gaussian processes [Bo and Sminchisescu, 2012]. While recent works explore computing or approximating the MI rule for quadratic functions [Bo and Sminchisescu, 2012, Thoppe et al., 2014], in general the MI rule is much more expensive than the GS rule.

2.2 Fixed vs. Variable Blocks

While the choice of the block to update has a significant effect on performance, how we define the set of *possible* blocks also has a major impact. Although other variations are possible, we highlight below the two most common blocking strategies:

1. **Fixed blocks.** This method uses a partition of the coordinates into disjoint blocks, as in our simple example above. This partition is typically chosen prior to the first iteration of the BCD algorithm, and this set of blocks is then held fixed for all iterations of the algorithm. We often use blocks of roughly equal size, so if we use blocks of size τ this method might partition the n coordinates into n/τ blocks. Generic ways to partition the coordinates include “in order” as we did above [Bertsekas, 2016], or using a random partition [Nesterov, 2010]. Alternatively, the partition may exploit some inherent substructure of the objective function such as block separability [Meier et al., 2008], the ability to efficiently solve the corresponding sub-problem (2) with respect to the blocks [Sardy et al., 2000], or based on the Lipschitz constants of the resulting blocks [Csiba and Richtárik, 2016, Thoppe et al., 2014].
2. **Variable blocks.** Instead of restricting our blocks to a pre-defined partition of the coordinates, we could instead consider choosing any of the $2^n - 1$ possible sets of coordinates as our block. In the randomized setting, this is referred to as “arbitrary” sampling [Qu and Richtárik, 2016, Richtárik and Takáč, 2016]. We say that such strategies use *variable* blocks because we are not choosing from a partition of the coordinates that is fixed across the iterations. Due to computational considerations, when using variable blocks we typically want to impose a restriction on the size of the blocks. For example, we could construct a block of size τ by randomly sampling τ coordinates without replacement, which is known as τ -nice sampling [Qu and Richtárik, 2016, Richtárik and Takáč, 2016]. Alternately, we could include each coordinate in the block b_k with some probability like τ/n (so the block size may change across iterations but we control its expected size). A version of the greedy Gauss-Southwell rule (4) with variable blocks would select the τ coordinates corresponding to the elements of the gradient with largest magnitudes [Tseng and Yun, 2009a]. This can be viewed as a greedy variant of τ -nice sampling. While we can find these τ coordinates easily, computing the MI rule with variable blocks is much more difficult. Indeed, while methods exist to compute the MI rule for quadratics with fixed blocks [Thoppe et al., 2014], with variable blocks it is NP-hard to compute the MI rule and existing works resort to approximations [Bo and Sminchisescu, 2012].

2.3 Block Update Rules

The selection of the update vector d^k can significantly affect performance of the BCD method. For example, in the gradient update (3) the method can be sensitive to the choice of the step-size α_k . Classic ways

to set α_k include using a fixed step-size (with each block possibly having its own fixed step-size), using an approximate line-search, or using the optimal step-size (which has a closed-form solution for quadratic objectives) [Bertsekas, 2016].

The most common alternative to the gradient update above is a **Newton update**,

$$d^k = -\alpha_k (\nabla_{b_k b_k}^2 f(x^k))^{-1} \nabla_{b_k} f(x^k), \quad (5)$$

where we might replace the instantaneous Hessian $\nabla_{b_k b_k}^2 f(x^k)$ by a positive-definite approximation to it. In this context the step-size α_k is again a step-size that can be chosen using similar strategies to those mentioned above. Several recent works analyze such updates and show that they can substantially improve the convergence rate [Fountoulakis and Tappenden, 2015, Qu et al., 2016, Tappenden et al., 2016]. For special problem classes, another possible type of update is what we will call the **optimal update**. This update chooses d^k to solve (2). In other words, it updates the block b_k to maximally decrease the objective function.

2.4 Problems of Interest

BCD methods tend to be good choices for problems where we can update all variables for roughly the same cost as computing the gradient. Two common classes of objective functions where single-coordinate descent methods tend to be suitable are thus

$$h_1(x) := \sum_{i=1}^n g_i(x_i) + f(Ax), \quad \text{or} \quad h_2(x) := \sum_{i \in V} g_i(x_i) + \sum_{(i,j) \in E} f_{ij}(x_i, x_j),$$

where f is smooth and cheap, the f_{ij} are smooth, $G = \{V, E\}$ is a graph, and A is a matrix [Nutini et al., 2015]. Examples of problems leading to functions of the form h_1 include least squares, logistic regression, LASSO, and SVMs.¹ The most important example of problem h_2 is quadratic functions, which are crucial to many aspects of scientific computing.²

Problems h_1 and h_2 are also suitable for BCD methods, as they tend to admit efficient block update strategies. In general, if single-coordinate descent is efficient for a problem, then BCD methods are also efficient for that problem and this applies whether we use fixed blocks or variable blocks. Other scenarios where coordinate descent and BCD methods have proven useful include matrix and tensor factorization methods [Xu and Yin, 2013, Yu et al., 2012], problems involving log-determinants [Hsieh et al., 2013, Scheinberg and Rish, 2009], and problems involving convex extensions of sub-modular functions [Ene and Nguyen, 2015, Jegelka et al., 2013].

An important point to note is that there are special problem classes where BCD with fixed blocks is reasonable even though using variable blocks (or single-coordinate updates) would not be suitable. For example, consider a variant of problem h_1 where we use *group* L1-regularization [Bakin, 1999],

$$h_3(x) := \sum_{b \in \mathcal{B}} \|x_b\| + f(Ax), \quad (6)$$

where \mathcal{B} is a partition of the coordinates. We cannot apply single-coordinate updates to this problem due to the non-smooth norms, but we can take advantage of the group-separable structure in the sum of norms and apply BCD using the blocks in \mathcal{B} [Meier et al., 2008, Qin et al., 2013]. Sardy et al. [2000] in their early work on solving LASSO problems consider problem h_1 where the columns of A are the union of a set of orthogonal matrices. By choosing the fixed blocks to correspond to the orthogonal matrices, it is very efficient to apply BCD. In appendix A, we outline how fixed blocks lead to an efficient greedy BCD method for the widely-used multi-class logistic regression problem when the data has a certain sparsity level.

¹Coordinate descent remains suitable for multi-linear generalizations of problem h_1 like functions of the form $f(XY)$ where X and Y are both matrix variables.

²Problem h_2 can be generalized to allow functions between more than 2 variables, and coordinate descent remains suitable as long as the expected number of functions in which each variable appears is n -times smaller than the total number of functions (assuming each function has a constant cost).

3 Improved Greedy Rules

Previous works have identified that the greedy GS rule can lead to suboptimal progress, and have proposed rules that are closer to the MI rule for the special case of quadratic functions [Bo and Sminchisescu, 2012, Thoppe et al., 2014]. However, for non-quadratic functions it is not obvious how we should approximate the MI rule. As an intermediate between the GS rule and the MI rule for general functions, a new rule known as the Gauss-Southwell-Lipschitz (GSL) rule has recently been introduced [Nutini et al., 2015]. The GSL rule was proposed in the case of single-coordinate updates, and is a variant of the GS rule that incorporates Lipschitz information to guarantee more progress per iteration. The GSL rule is equivalent to the MI rule in the special case of quadratic functions, so either rule can be used in that setting. However, the MI rule involves optimizing over a subspace which will typically be expensive for non-quadratic functions. After reviewing the classic block GS rule, in this section we consider several possible block extensions of the GSL rule that give a better approximation to the MI rule without requiring subspace optimization.

3.1 Block Gauss-Southwell

When analyzing BCD methods we typically assume that the gradient of each block b is L_b -Lipschitz continuous, meaning that for all $x \in \mathbb{R}^n$ and $d \in \mathbb{R}^{|b|}$

$$\|\nabla_b f(x + U_b d) - \nabla_b f(x)\| \leq L_b \|d\|, \quad (7)$$

for some constant $L_b > 0$. This is a standard assumption, and in appendix B we give bounds on L_b for the common data-fitting models of least squares and logistic regression. If we apply the descent lemma [Bertsekas, 2016] to the reduced sub-problem (2) associated with some block b_k selected at iteration k , then we obtain the following upper bound on the function value progress,

$$\begin{aligned} f(x^{k+1}) &\leq f(x^k) + \langle \nabla f(x^k), x^{k+1} - x^k \rangle + \frac{L_{b_k}}{2} \|x^{k+1} - x^k\|^2 \\ &= f(x^k) + \langle \nabla_{b_k} f(x^k), d^k \rangle + \frac{L_{b_k}}{2} \|d^k\|^2. \end{aligned} \quad (8)$$

The right side is minimized in terms of d^k under the choice

$$d^k = -\frac{1}{L_{b_k}} \nabla_{b_k} f(x^k), \quad (9)$$

which is simply a gradient update with a step-size of $\alpha_k = 1/L_{b_k}$. Substituting this into our upper bound, we obtain

$$f(x^{k+1}) \leq f(x^k) - \frac{1}{2L_{b_k}} \|\nabla_{b_k} f(x^k)\|_2. \quad (10)$$

A reasonable way to choose a block b_k at each iteration is by minimizing the upper bound in (10) with respect to b_k . For example, if we assume that L_b is the same for all blocks b then we derive the GS rule (4) of choosing the b_k that maximizes the gradient norm.

We can use the bound (10) to compare the progress made by different selection rules. For example, this bound indicates that the GS rule can make more progress with variable blocks than with fixed blocks (under the usual setting where the fixed blocks are a subset of the possible variable blocks). In particular, consider the case where we have partitioned the coordinates into blocks of size τ and we are comparing this to using variable blocks of size τ . The case where there is no advantage for variable blocks is when the indices corresponding to the τ -largest $|\nabla_i f(x^k)|$ values are in one of the fixed partitions; in this (unlikely) case the GS rule with fixed blocks and variable blocks will choose the same variables to update. The case where we see the largest advantage of using variable blocks is when each of the indices corresponding to the τ -largest $|\nabla_i f(x^k)|$ values are in different blocks of the fixed partition; in this case the last term in (10) can be improved by a factor as large as τ^2 when using variable blocks instead of fixed blocks. Thus, with larger blocks there is more of an advantage to using variable blocks over fixed blocks.

3.2 Block Gauss-Southwell-Lipschitz

The GS rule is not the optimal block selection rule in terms of the bound (10) if we know the block-Lipschitz constants L_b . Instead of choosing the block with largest norm, consider minimizing (10) in terms of b_k ,

$$b_k \in \arg \max_{b \in \mathcal{B}} \left\{ \frac{\|\nabla_b f(x^k)\|^2}{L_b} \right\}. \quad (11)$$

We call this the **block Gauss-Southwell-Lipschitz** (GSL) rule. If all L_b are the same, then the GSL rule is equivalent to the classic GS rule. But in the typical case where the L_b differ, the GSL rule guarantees more progress than the GS rule since it incorporates the gradient information as well as the Lipschitz constants L_b . For example, it reflects that if the gradients of two blocks are similar but their Lipschitz constants are very different, then we can guarantee more progress by updating the block with the smaller Lipschitz constant. In the extreme case, for both fixed and variable blocks the GSL rule improves the bound (10) over the GS rule by a factor as large as $(\max_{b \in \mathcal{B}} L_b)/(\min_{b \in \mathcal{B}} L_b)$.

The block GSL rule in (11) is a simple generalization of the single-coordinate GSL rule to blocks of any size. However, it loses a key feature of the single-coordinate GSL rule: the block GSL rule is *not* equivalent to the MI rule for quadratic functions. Unlike the single-coordinate case, where $\nabla_{ii}^2 f(x^k) = L_i$ so that (8) holds with equality, for the block case we only have $\nabla_{bb}^2 f(x^k) \preceq L_b$ so (8) may underestimate the progress that is possible in certain directions. In the next section we give a second generalization of the GSL rule that is equivalent to the MI rule for quadratics.

3.3 Block Gauss-Southwell-Quadratic

For single-coordinate updates, the bound in (10) is the tightest quadratic bound on progress we can expect given only the assumption of block Lipschitz-continuity (it holds with equality for quadratic functions). However, for block updates of more than one variable we can obtain a tighter quadratic bound using general quadratic norms of the form $\|\cdot\|_H = \sqrt{\langle H \cdot, \cdot \rangle}$ for some positive-definite matrix H . In particular, assume that each block has a Lipschitz-continuous gradient with $L_b = 1$ for a particular positive-definite matrix $H_b \in \mathbb{R}^{|b| \times |b|}$, meaning that

$$\|\nabla_b f(x + U_b d) - \nabla_b f(x)\|_{H_b^{-1}} \leq \|d\|_{H_b},$$

for all $x \in \mathbb{R}^n$ and $d \in \mathbb{R}^{|b|}$. Due to the equivalence between norms, this merely changes how we measure the continuity of the gradient and is not imposing any new assumptions. Indeed, the block Lipschitz-continuity assumption in (7) is just a special case of the above with $H_b = L_b I$, where I is the $|b| \times |b|$ identity matrix. Although this characterization of Lipschitz continuity appears more complex, for some functions it is actually computationally cheaper to construct matrices H_b than to find valid bounds L_b . We show this in appendix B for the cases of least squares and logistic regression.

Under this alternative characterization of the Lipschitz assumption, at each iteration k we have

$$f(x^{k+1}) \leq f(x^k) + \langle \nabla_{b_k} f(x^k), d^k \rangle + \frac{1}{2} \|d^k\|_{H_{b_k}}^2. \quad (12)$$

The left-hand side of (12) is minimized when

$$d^k = -(H_{b_k})^{-1} \nabla_{b_k} f(x^k), \quad (13)$$

which we will call the **matrix update** of a block. Although this is equivalent to Newton’s method for quadratic functions, we use the name “matrix update” rather than “Newton’s method” here to distinguish two types of updates: Newton’s method is based on the instantaneous Hessian $\nabla_{bb}^2 f(x^k)$, while the matrix update is based on a matrix H_b that upper bounds the Hessian for all x .³ We will discuss Newton updates in subsequent sections, but substituting the matrix update into the upper bound yields

$$f(x^{k+1}) \leq f(x^k) - \frac{1}{2} \|\nabla_{b_k} f(x^k)\|_{H_{b_k}^{-1}}^2. \quad (14)$$

³We say that a matrix A “upper bounds” a matrix B , written $A \succeq B$, if for all x we have $x^T A x \geq x^T B x$.

Consider a simple quadratic function $f(x) = x^T A x$ for a positive-definite matrix A . In this case we can take H_b to be the sub-matrix A_{bb} while in our previous bound we would require L_b to be the maximum eigenvalue of this sub-matrix. Thus, in the worst case (where $\nabla_{b_k} f(x^k)$ is in the span of the principal eigenvectors of A_{bb}) the new bound is at least as good as (10). But if the eigenvalues of A_{bb} are spread out then this bound shows that the matrix update will typically guarantee substantially more progress; in this case the quadratic bound (14) can improve on the bound in (10) by a factor as large as the condition number of A_{bb} when updating block b . The update (13) was analyzed for BCD methods in several recent works [Qu et al., 2016, Tappenden et al., 2016], which considered random selection of the blocks. They show that this update provably reduces the number of iterations required, and in some cases dramatically. For the special case of quadratic functions where (14) holds with equality, greedy rules based on minimizing this bound have been explored for both fixed [Thoppe et al., 2014] and variable [Bo and Sminchisescu, 2012] blocks.

Rather than focusing on the special case of quadratic functions, we want to define a better greedy rule than (11) for functions with Lipschitz-continuous gradients. By optimizing (14) in terms of b_k we obtain a second generalization of the GSL rule,

$$b_k \in \arg \max_{b \in \mathcal{B}} \left\{ \|\nabla_b f(x^k)\|_{H_b^{-1}} \right\} \equiv \arg \max_{b \in \mathcal{B}} \left\{ \nabla_b f(x^k)^T H_b^{-1} \nabla_b f(x^k) \right\}, \quad (15)$$

which we call the **block Gauss-Southwell quadratic** (GSQ) rule.⁴ Since (14) holds with equality for quadratics this new rule is equivalent to the MI rule in that case. But this rule also applies to non-quadratic functions where it guarantees a better bound on progress than the GS rule (and the GSL rule).

3.4 Block Gauss-Southwell-Diagonal

While the GSQ rule has appealing theoretical properties, for many problems it may be difficult to find full matrices H_b and their storage may also be an issue. Previous related works [Csiba and Richtárik, 2017, Qu et al., 2016, Tseng and Yun, 2009a] address this issue by restricting the matrices H_b to be diagonal matrices D_b . Under this choice we obtain a rule of the form

$$b_k \in \arg \max_{b \in \mathcal{B}} \left\{ \|\nabla_b f(x^k)\|_{D_b^{-1}} \right\} \equiv \arg \max_{b \in \mathcal{B}} \left\{ \sum_{i \in b} \frac{|\nabla_i f(x^k)|^2}{D_{b,i}} \right\}, \quad (16)$$

where we are using $D_{b,i}$ to refer to the diagonal element corresponding to coordinate i in block b . We call this the **block Gauss-Southwell diagonal** (GSD) rule. This bound arises if we consider a gradient update, where coordinate i has a constant step-size of $D_{b,i}^{-1}$ when updated as part of block b . This rule gives an intermediate approach that can guarantee more progress per iteration than the GSL rule, but that may be easier to implement than the GSQ rule.

3.5 Convergence Rate under Polyak-Łojasiewicz

Our discussion above focuses on the progress we can guarantee at each iteration, assuming only that the function has a Lipschitz-continuous gradient. Under additional assumptions, it is possible to use these progress bounds to derive convergence rates on the overall BCD method. For example, we say that a function f satisfies the Polyak-Łojasiewicz (PL) inequality [Polyak, 1963] if for all x we have for some $\mu > 0$ that

$$\frac{1}{2} (\|\nabla f(x)\|_*)^2 \geq \mu (f(x) - f^*), \quad (17)$$

where $\|\cdot\|_*$ can be any norm and f^* is the optimal function value. The function class satisfying this inequality includes all strongly-convex functions but also includes a variety of other important problems like

⁴While preparing this work for submission, we were made aware of a work that independently proposed this rule under the name “greedy mini-batch” rule [Csiba and Richtárik, 2017]. However, our focus on addressing the computational issues associated with the rule is quite different from that work, which focuses on tight convergence analyses.

least squares [Karimi et al., 2016]. This inequality leads to a simple proof of the linear convergence of any algorithm which has a progress bound of the form

$$f(x^{k+1}) \leq f(x^k) - \frac{1}{2} \|\nabla f(x^k)\|_*^2, \quad (18)$$

such as gradient descent or coordinate descent with the GS rule [Karimi et al., 2016].

Theorem 1. *Assume f satisfies the PL-inequality (17) for some $\mu > 0$ and norm $\|\cdot\|_*$. Any algorithm that satisfies a progress bound of the form (18) with respect to the same norm $\|\cdot\|_*$ obtains the following linear convergence rate,*

$$f(x^{k+1}) - f^* \leq (1 - \mu)^k [f(x^0) - f^*]. \quad (19)$$

Proof. By subtracting f^* from both sides of (18) and applying (17) directly, we obtain our result by recursion. \square

Thus, if we can describe the progress obtained using a particular block selection rule and block update rule in the form of (18), then we have a linear rate of convergence for BCD on this class of functions. It is straightforward to do this using an appropriately defined norm, as shown in the following corollary.

Corollary 1. *Assume ∇f is Lipschitz continuous (12) and that f satisfies the PL-inequality (17) in the norm defined by*

$$\|v\|_{\mathcal{B}} = \max_{b \in \mathcal{B}} \|v_b\|_{H_{b^{-1}}}, \quad (20)$$

for some $\mu > 0$ and matrix $H_b \in \mathbb{R}^{b \times b}$. Then the BCD method using either the GSQ, GSL, GSD or GS selection rule achieves a linear convergence rate of the form (19).

Proof. Using the definition of the GSQ rule (15) in the progress bound resulting from the Lipschitz continuity of ∇f and the matrix update (14), we have

$$\begin{aligned} f(x^{k+1}) &\leq f(x^k) - \frac{1}{2} \max_{b \in \mathcal{B}} \left\{ \|\nabla_b f(x^k)\|_{H_b^{-1}}^2 \right\} \\ &= f(x^k) - \frac{1}{2} \|\nabla f(x^k)\|_{\mathcal{B}}^2. \end{aligned} \quad (21)$$

By Theorem 1 and the observation that the GSL, GSD and GS rules are all special cases of the GSQ rule corresponding to specific choices of H_b , we have our result. \square

We refer the reader to the work of Csiba and Richtárik for tools that allow alternative analyses of BCD methods [Csiba and Richtárik, 2017].

3.6 Convergence Rate with General Functions

The PL inequality is satisfied for many problems of practical interest, and is even satisfied for some non-convex functions. However, general non-convex functions do not satisfy the PL inequality and thus the analysis of the previous section does not apply. Without a condition like the PL inequality, it is difficult to show convergence to the optimal function value f^* (since we should not expect a local optimization method to be able to find the global solution of functions that may be NP-hard to minimize). However, the bound (21) still implies a weaker type of convergence rate even for general non-convex problems. The following result is a generalization of a standard argument for the convergence rate of gradient descent [Nesterov, 2004], and gives us an idea of how fast the BCD method is able to find a point resembling a stationary point even in the general non-convex setting.

Theorem 2. *Assume ∇f is Lipschitz continuous (12) and that f is bounded below by some f^* . Then the BCD method using either the GSQ, GSL, GSD or GS selection rule achieves the following convergence rate of the minimum gradient norm,*

$$\min_{t=0,1,\dots,k-1} \|\nabla f(x^t)\|_{\mathcal{B}}^2 \leq \frac{2(f(x^0) - f^*)}{k}.$$

Proof By rearranging (21), we have

$$\frac{1}{2} \|\nabla f(x^k)\|_{\mathcal{B}}^2 \leq f(x^k) - f(x^{k+1}).$$

Summing this inequality over iterations $t = 0$ up to $(k - 1)$ yields

$$\frac{1}{2} \sum_{t=0}^{k-1} \|\nabla f(x^t)\|_{\mathcal{B}}^2 \leq f(x^0) - f(x^{k+1}).$$

Using that all k elements in the sum are lower bounded by their minimum and that $f(x^{k+1}) \geq f^*$, we get

$$\frac{k}{2} \left(\min_{t=0,1,\dots,k-1} \|\nabla f(x^t)\|_{\mathcal{B}}^2 \right) \leq f(x^0) - f^*. \quad \square$$

Due to the potential non-convexity we cannot say anything about the gradient norm of the final iteration, but this shows that the minimum gradient norm converges to zero with an error at iteration k of $O(1/k)$. This is a global sublinear result, but note that if the algorithm eventually arrives and stays in a region satisfying the PL inequality around a set of local optima, then the local convergence rate to this set of optima will increase to be linear.

4 Practical Issues

The previous section defines straightforward new rules that yield a simple analysis. In practice there are several issues that remain to be addressed. For example, it seems intractable to compute any of the new rules in the case of variable blocks. Furthermore, we may not know the Lipschitz constants for our problem. For fixed blocks we also need to consider how to partition the coordinates into blocks. Another issue is that the d^k choices used above do not incorporate the local Hessian information. Although how we address these issues will depend on our particular application, in this section we discuss several issues associated with these practical considerations.

4.1 Tractable GSD for Variable Blocks

The problem with using any of the new selection rules above in the case of variable blocks is that they seem intractable to compute for any non-trivial block size. In particular, to compute the GSL rule using variable blocks requires the calculation of L_b for each possible block, which seems intractable for any problem of reasonable size. Since the GSL rule is a special case of the GSD and GSQ rules, these rules also seem intractable in general. In this section we show how to restrict the GSD matrices so that this rule has the same complexity as the classic GS rule.

Consider a variant of the GSD rule where each $D_{b,i}$ can depend on i but does not depend on b , so we have $D_{b,i} = d_i$ for some value $d_i \in \mathbb{R}_+$ for all blocks b . This gives a rule of the form

$$b_k \in \arg \max_{b \in \mathcal{B}} \left\{ \sum_{i \in b} \frac{|\nabla_i f(x^k)|^2}{d_i} \right\}. \quad (22)$$

Unlike the general GSD rule, this rule has essentially the same complexity as the classic GS rule since it simply involves finding the largest values of the ratio $|\nabla_i f(x^k)|^2/d_i$.

A natural choice of the d_i values would seem to be $d_i = L_i$, since in this case we recover the GSL rule if the blocks have a size of 1 (here we are using L_i to refer to the coordinate-wise Lipschitz constant of coordinate i). Unfortunately, this does not lead to a bound of the form (18) as needed in Theorems 1 and 2 because coordinate-wise L_i -Lipschitz continuity with respect to the Euclidean norm does not imply 1-Lipschitz continuity with respect to the norm $\|\cdot\|_{D_b^{-1}}$ when the block size is larger than 1. Subsequently,

the steps under this choice may increase the objective function. A similar restriction on the D_b matrices in (22) is used in the implementation of Tseng and Yun based on the Hessian diagonals [Tseng and Yun, 2009a], but their approach similarly does not give an upper bound and thus they employ a line search in their block update.

It is possible to avoid needing a line search by setting $D_{b,i} = L_i\tau$, where τ is the maximum block size in \mathcal{B} . This still generalizes the single-coordinate GSL rule, and in appendix C we show that this leads to a bound of the form (18) for twice-differentiable convex functions (thus Theorems 1 and 2 hold). If all blocks have the same size then this approach selects the same block as using $D_{b,i} = L_i$, but the matching block update uses a much-smaller step-size that guarantees descent. We do not advocate using this smaller step, but note that the bound we derive also holds for alternate updates like taking a gradient update with $\alpha_k = 1/L_{b_k}$ or using a matrix update based on H_{b_k} .

The choice of $D_{b,i} = L_i\tau$ leads to a fairly pessimistic bound, but it is not obvious even for simple problems how to choose an optimal set of D_i values. Choosing these values is related to the problem of finding an expected separable over-approximation (ESO), which arises in the context of randomized coordinate descent methods [Richtárik and Takáč, 2016]. Qu and Richtárik give an extensive discussion of how we might bound such quantities for certain problem structures [Qu and Richtárik, 2016]. In our experiments we also explored another simple choice that is inspired by the “simultaneous iterative reconstruction technique” (SIRT) from tomographic image reconstruction [Gregor and Fessler, 2015]. In this approach, we use a matrix upper bound M on the full Hessian $\nabla^2 f(x)$ (for all x) and set⁵

$$D_{b,i} = \sum_{j=1}^n |M_{i,j}|. \quad (23)$$

We found that this choice worked better when using gradient updates, although using the simpler $L_i\tau$ is less expensive and was more effective when doing matrix updates.

By using the relationship $L_b \leq \sum_{i \in b} L_i \leq |b| \max_{i \in b} L_i$, two other ways we might consider defining a more-tractable rule could be

$$b_k \in \arg \max_{b \in \mathcal{B}} \left\{ \frac{\sum_{i \in b} |\nabla_i f(x^k)|^2}{|b| \max_{i \in b} L_i} \right\}, \quad \text{or} \quad b_k \in \arg \max_{b \in \mathcal{B}} \left\{ \frac{\sum_{i \in b} |\nabla_i f(x^k)|^2}{\sum_{i \in b} L_i} \right\}.$$

The rule on the left can be computed using dynamic programming while the rule on the right can be computed using an algorithm of Megiddo [1979]. However, when using a step-size of $1/L_b$ we found both rules performed similarly or worse to using the GSD rule with $D_{i,b} = L_i$ (when paired with gradient or matrix updates).⁶

4.2 Tractable GSQ for Variable Blocks

In order to make the GSQ rule tractable with variable blocks, we could similarly require that the entries of H_b depend solely on the coordinates $i \in b$, so that $H_b = M_{b,b}$ where M is a fixed matrix (as above) and $M_{b,b}$ refers to the sub-matrix corresponding to the coordinates in b . Our restriction on the GSD rule in the previous section corresponds to the case where M is diagonal. In the full-matrix case, the block selected according to this rule is given by the coordinates corresponding to the non-zero variables of an L0-constrained quadratic minimization,

$$\arg \min_{\|d\|_0 \leq \tau} \left\{ f(x^k) + \langle \nabla f(x^k), d \rangle + \frac{1}{2} d^T M d \right\}, \quad (24)$$

where $\|\cdot\|_0$ is the number of non-zeroes. This selection rule is discussed in Tseng and Yun [2009a], but in their implementation they use a diagonal M . Although this problem is NP-hard with a non-diagonal M , there is a

⁵It follows that $D - M \succeq 0$ because it is symmetric and diagonally-dominant with non-negative diagonals.

⁶On the other hand, the rule on the right worked better if we forced the algorithms to use a step-size of $1/(\sum_{i \in b} L_i)$. But this led to worse performance overall than using the larger $1/L_b$ step-size.

recent wealth of literature on algorithms for finding approximate solutions. For example, one of the simplest local optimization methods for this problem is the iterative hard-thresholding (IHT) method [Blumensath and Davies, 2009]. Another popular method for approximately solving this problem is the orthogonal matching pursuit (OMP) method from signal processing which is also known as forward selection in statistics [Hocking, 1976, Pati et al., 1993]. Computing d via (24) is also equivalent to computing the MI rule for a quadratic function, and thus we could alternately use the approximation of Bo and Sminchisescu [2012] for this problem.

Although it appears quite general, note that the exact GSQ rule under this restriction on H_b does not guarantee as much progress as the more-general GSQ rule (if computed exactly) that we proposed in the previous section. For some problems we can obtain tighter matrix bounds over blocks of variables than are obtained by taking the sub-matrix of a fixed matrix-bound over all variables. We show this for the case of multi-class logistic regression in appendix B. As a consequence of this result we conclude that there does not appear to be a reason to use this restriction in the case of fixed blocks.

Although using the GSQ rule with variable blocks forces us to use an approximation, these approximations might still select a block that makes more progress than methods based on diagonal approximations (which ignore the strengths of dependencies between variables). It is possible that approximating the GSQ rule does not necessarily lead to a bound of the form (18) as there may be no fixed norm for which this inequality holds. However, in this case we can initialize the algorithm with an update rule that does achieve such a bound in order to guarantee that Theorems 1 and 2 hold, since this initialization ensures that we do at least as well as this reference block selection rule.

The main disadvantage of this approach for large-scale problems is the need to deal with the full matrix M (which does not arise when using a diagonal approximation or using fixed blocks). In large-scale settings we would need to consider matrices M with special structures like the sum of a diagonal matrix with a sparse and/or a low-rank matrix.

4.3 Lipschitz Estimates for Fixed Blocks

Using the GSD rule with the choice of $D_{i,b} = L_i$ may also be useful in the case of fixed blocks. In particular, if it is easier to compute the single-coordinate L_i values than the block L_b values then we might prefer to use the GSD rule with this choice. On the other hand, an appealing alternative in the case of fixed blocks is to use an estimate of L_b for each block as in Nesterov’s work [Nesterov, 2010]. In particular, for each L_b we could start with some small estimate (like $L_b = 1$) and then double it whenever the inequality (10) is not satisfied (since this indicates L_b is too small). Given some b , the bound obtained under this strategy is at most a factor of 2 slower than using the optimal values of L_b . Further, if our estimate of L_b is much smaller than the global value, then this strategy can actually guarantee much more progress than using the “correct” L_b value.⁷

In the case of matrix updates, we can use (14) to verify that an H_b matrix is valid [Fountoulakis and Tappenden, 2015]. Recall that (14) is derived by plugging the update (13) into the Lipschitz progress bound (12). Unfortunately, it is not obvious how to update a matrix H_b if we find that it is not a valid upper bound. One simple possibility is to multiply the elements of our estimate H_b by 2. This is equivalent to using a matrix update but with a scalar step-size α_k ,

$$d^k = -\alpha_k(H_b)^{-1}\nabla_{b_k}f(x^k), \tag{25}$$

similar to the step-size in the Newton update (5).

4.4 Efficient Line-Searches

The Lipschitz approximation procedures of the previous section do not seem practical when using variable blocks, since there are an exponential number of possible blocks. To use variable blocks for problems where we do not know L_b or H_b , a reasonable approach is to use a line-search. For example, we can choose α_k

⁷While it might be tempting to also apply such estimates in the case of variable blocks, a practical issue is that we would need a step-size for all of the exponential number of possible variable blocks.

in (25) using a standard line-search like those that use the Armijo condition or Wolfe conditions [Nocedal and Wright, 1999]. When using large block sizes with gradient updates, line-searches based on the Wolfe conditions are likely to make more progress than using the *true* L_b values (since for large block sizes the line-search would tend to choose values of α_k that are much larger than $\alpha_k = 1/L_{b_k}$).

Further, the problem structures that lend themselves to efficient coordinate descent algorithms tend to lend themselves to efficient line-search algorithms. For example, if our objective has the form $f(Ax)$ then a line-search would try to minimize the $f(Ax^k + \alpha_k AU_{b_k} d^k)$ in terms of α_k . Notice that the algorithm would already have access to Ax^k and that we can efficiently compute $AU_{b_k} d^k$ since it only depends on the columns of A that are in b_k . Thus, after (efficiently) computing $AU_{b_k} d^k$ once the line-search simply involves trying to minimize $f(v_1 + \alpha_k v_2)$ in terms of α_k (for particular vectors v_1 and v_2). The cost of this approximate minimization will typically not add a large cost to the overall algorithm.

4.5 Block Partitioning with Fixed Blocks

Several prior works note that for fixed blocks the partitioning of coordinates into blocks can play a significant role in the performance of BCD methods. Thoppe et al. [2014] suggest trying to find a block-diagonally dominant partition of the coordinates, and experimented with a heuristic for quadratic functions where the coordinates corresponding to the rows with the largest values were placed in the same block. In the context of parallel BCD, Scherrer et al. [2012] consider a feature clustering approach in the context of problem h_1 that tries to minimize the spectral norm between columns of A from different blocks. Csiba and Richtárik [2016] discuss strategies for partitioning the coordinates when using randomized selection.

Based on the discussion in the previous sections, for greedy BCD methods it is clear that we guarantee the most progress if we can make the mixed norm $\|\nabla f(x^k)\|_{\mathcal{B}}$ as large as possible *across iterations* (assuming that the H_b give a valid bound). This supports strategies where we try to minimize the maximum Lipschitz constant across iterations. One way to do this is to try to ensure that the average Lipschitz constant across the blocks is small. For example, we could place the largest L_i value with the smallest L_i value, the second-largest L_i value with the second-smallest L_i value, and so on. While intuitive, this may be sub-optimal; it ignores that if we cleverly partition the coordinates we may force the algorithm to often choose blocks with very-small Lipschitz constants (which lead to much more progress in decreasing the objective function). In our experiments, similar to the method of Thoppe et. al. for quadratics, we explore the simple strategy of *sorting the L_i values and partitioning this list into equal-sized blocks*. Although in the worst case this leads to iterations that are not very productive since they update all of the largest L_i values, it also guarantees some very productive iterations that update none of the largest L_i values and leads to better overall performance in our experiments.

4.6 Newton Updates

Choosing the vector d^k that we use to update the block x_{b_k} would seem to be straightforward since in the previous section we derived the block selection rules in the context of specific block updates; the GSL rule is derived assuming a gradient update (9), the GSQ rule is derived assuming a matrix update (13), and so on. However, using the update d^k that leads to the selection rule can be highly sub-optimal. For example, we might make substantially more progress using the matrix update (13) even if we choose the block b_k based on the GSL rule. Indeed, given b_k the matrix update makes the optimal amount of progress for quadratic functions, so in this case we should prefer the matrix update for all selection rules (including random and cyclic rules).

However, the matrix update in (13) can itself be highly sub-optimal for non-quadratic functions as it employs an upper-bound H_{b_k} on the sub-Hessian $\nabla_{b_k b_k}^2 f(x)$ that must hold for *all* parameters x . For twice-differentiable non-quadratic functions, we could potentially make more progress by using classic Newton updates where we use the instantaneous Hessian $\nabla_{b_k b_k}^2 f(x^k)$ with respect to the block. Indeed, considering the extreme case where we have one block containing all the coordinates, Newton updates can lead to superlinear convergence [Dennis and Moré, 1974] while matrix updates destroy this property. That being

said, we should not expect superlinear convergence of BCD methods with Newton or even optimal updates⁸. Nevertheless, in Section 6 we show that for certain common problem structures it’s possible to achieve superlinear convergence with Newton-style updates.

Fountoulakis & Tappenden recently highlight this difference between using matrix updates and using Newton updates [Fountoulakis and Tappenden, 2015], and propose a BCD method based on Newton updates. To guarantee progress when far from the solution classic Newton updates require safeguards like a line-search or trust-region [Fountoulakis and Tappenden, 2015, Tseng and Yun, 2009a], but as we’ve discussed in this section line-searches tend not to add a significant cost to BCD methods. Thus, if we want to maximize the progress we make at each iteration we recommend to use one of the greedy rules to select the block to update, but then update the block using the Newton direction and a line-search. In our implementation, we used a backtracking line-search starting with $\alpha_k = 1$ and backtracking for the first time using quadratic Hermite polynomial interpolation and using cubic Hermite polynomial interpolation if we backtracked more than once (which rarely happened since $\alpha_k = 1$ or the first backtrack were typically accepted) [Nocedal and Wright, 1999].⁹

5 Message-Passing for Huge-Block Updates

Qu et al. [2016] discuss how in some settings increasing the block size with matrix updates does not necessarily lead to a performance gain due to the higher iteration cost. In the case of Newton updates the additional cost of computing the sub-Hessian $\nabla_{bb}^2 f(x^k)$ may also be non-trivial. Thus, whether matrix and Newton updates will be beneficial over gradient updates will depend on the particular problem and the chosen block size. However, in this section we argue that in some cases matrix updates and Newton updates can be computed efficiently using huge blocks. In particular, we focus on the case where the dependencies between variables are sparse, and we will choose the structure of the blocks in order to guarantee that the matrix/Newton update can be computed efficiently.

The cost of using Newton updates with the BCD method depends on two factors: (i) the cost of calculating the sub-Hessian $\nabla_{bb}^2 f(x^k)$ and (ii) the cost of solving the corresponding linear system. The cost of computing the sub-Hessian depends on the particular objective function we are minimizing. But, for the problems where coordinate descent is efficient (see Section 2.4), it is typically substantially cheaper to compute the sub-Hessian for a block than to compute the full Hessian. Indeed, for many cases where we apply BCD, computing the sub-Hessian for a block is cheap due to the sparsity of the Hessian. For example, in the graph-structured problems h_2 the edges in the graph correspond to the non-zeroes in the Hessian.

Although this sparsity and reduced problem size would seem to make BCD methods with exact Newton updates ideal, in the worst case the iteration cost would still be $O(|b_k|^3)$ using standard matrix factorization methods. A similar cost is needed using the matrix updates with fixed Hessian upper-bounds H_b and for performing an optimal update in the special case of quadratic functions. In some settings we can reduce this to $O(|b_k|^2)$ by storing matrix factorizations, but this cost is still prohibitive if we want to use large blocks (we can use $|b_k|$ in the thousands but not the millions).

An alternative to computing the exact Newton update is to use an approximation to the Newton update that has a runtime dominated by the sparsity level of the sub-Hessian. For example, we could use conjugate gradient methods or use randomized Hessian approximations [Dembo et al., 1982, Pilanci and Wainwright, 2017]. However, these approximations require setting an approximation accuracy and may be inaccurate if the sub-Hessian is not well-conditioned. In this section we consider an alternative approach: choosing blocks with a sparsity pattern that guarantees we can solve the resulting linear systems involving the sub-Hessian (or its approximation) in $O(|b_k|)$ using a “message-passing” algorithm. If the sparsity pattern is favourable, this allows us to update huge blocks at each iteration using exact matrix updates or Newton updates (which

⁸Consider a 2-variable quadratic objective where we use single-coordinate updates. The optimal update (which is equivalent to the matrix/Newton update) is easy to compute, but if the quadratic is non-separable then the convergence rate of this approach is only linear.

⁹We also explored a variant based on cubic regularization of Newton’s method [Nesterov and Polyak, 2006], but were not able to obtain a significant performance gain with this approach.

are the optimal updates for quadratic problems).

To illustrate the message-passing algorithm, we first consider the basic quadratic minimization problem

$$\arg \min_{x \in \mathbb{R}^n} \frac{1}{2} x^T A x - c^T x,$$

where we assume the matrix $A \in \mathbb{R}^{n \times n}$ is positive-definite and sparse. By excluding terms not depending on the coordinates in the block, the optimal update for block b is given by the solution to the linear system

$$A_{bb} x_b = \tilde{c}, \tag{26}$$

where $A_{bb} \in \mathbb{R}^{|b| \times |b|}$ is the submatrix of A corresponding to block b , and $\tilde{c} = c_b - A_{b\bar{b}} x_{\bar{b}}$ is a vector with \bar{b} defined as the complement of b and $A_{b\bar{b}} \in \mathbb{R}^{|b| \times |\bar{b}|}$ is the submatrix of A with rows from b and columns from \bar{b} . We note that in practice efficient BCD methods already need to track Ax so computing \tilde{c} is efficient. Although we focus on solving (26) for simplicity, the message-passing solution we discuss here will also apply to matrix updates (which leads to a linear system involving H_b) and Newton updates (which leads to a linear system involving the sub-Hessian).

Consider a pairwise undirected graph $G = (V, E)$, where the vertices V are the coordinates of our problem and the edges E are the non-zero off-diagonal elements of A . Thus, if A is diagonal then G has no edges, if A is dense then there are edges between all nodes (G is fully-connected), if A is tridiagonal then edges connect adjacent nodes (G is a chain-structured graph where $(1) - (2) - (3) - (4) - \dots$), and so on.

For BCD methods, unless we have a block size $|b| = n$, we only work with a subset of nodes b at each iteration. The graph obtained from the sub-matrix A_{bb} is called the *induced subgraph* G_b . Specifically, the nodes $V_b \in G_b$ are the coordinates in the set b , while the edges $E_b \in G_b$ are all edges $(i, j) \in E$ where $i, j \in V_b$ (edges between nodes in b). We are interested in the special case where the induced subgraph G_b forms a *forest*, meaning that it has no cycles.¹⁰ In the special case of forest-structured induced subgraphs, we can compute the optimal update (26) in linear time using message passing [Shental et al., 2008] instead of the cubic worst-case time required by typical matrix factorization implementations. Indeed, in this case the message passing algorithm is equivalent to Gaussian elimination [Bickson, 2009, Prop. 3.4.1] where the amount of “fill-in” is guaranteed to be linear. This idea of exploiting tree structures within Gaussian elimination dates back over 50 years [Parter, 1961], and similar ideas have recently been explored by Srinivasan and Todorov [2015] for Newton methods. Their *graphical Newton* algorithm can solve the Newton system in $O(t^3)$ times the size of G , where t is the “treewidth” of the graph ($t = 1$ for forests). However, the tree-width of G is usually large while it is more reasonable to assume that we can find low-treewidth induced subgraphs G_b .

To illustrate the message-passing algorithm in the terminology of Gaussian elimination, we first need to divide the nodes $\{1, 2, \dots, |b|\}$ in the forest into sets $L\{1\}, L\{2\}, \dots, L\{T\}$, where $L\{1\}$ is an arbitrary node in graph G_b selected to be the root node, $L\{2\}$ is the set of all neighbours of the “root” node, $L\{3\}$ is the set of all neighbours of the nodes in $L\{2\}$ excluding parent nodes (nodes in $L\{1:2\}$), and so on until all nodes are assigned to a set (if the forest is made of disconnected trees, we’ll need to do this for each tree). An example of this process is depicted in Figure 5. Once these sets are initialized, we start with the nodes furthest from the root node $L\{T\}$, and carry out the row operations of Gaussian elimination moving towards the root. Then we use backward substitution to solve the system $\tilde{A}x = \tilde{c}$. We outline the full procedure in Algorithm 1.

Whether or not message-passing is useful will depend on the sparsity pattern of A . For example, consider a quadratic function with a lattice-structured non-zero pattern as in Figure 3. A classic fixed partitioning strategy for problems with this common structure is to use a “red-black ordering” (see Figure 3a), where on each iteration we either update all of the red nodes or we update all of the black nodes. Choosing this graph colouring makes the matrix A_{bb} diagonal when we update the red nodes (and similarly for the black nodes), allowing us to solve (26) in linear time. So these blocks allow an optimal BCD update with a block

¹⁰An undirected cycle is a sequence of adjacent nodes in V starting and ending at the same node, where there are no repetitions of nodes or edges other than the final node.

Algorithm 1 Message Passing for a Tree Graph

1. **Initialize:**
 Input: vector \tilde{c} , forest-structured matrix \tilde{A} , and levels $L\{1\}, L\{2\}, \dots, L\{T\}$.
for $i = 1, 2, \dots, |b|$
 Set $P_{ii} \leftarrow \tilde{A}_{ii}, C_i \leftarrow \tilde{c}_i$. # P, C track row operations

 2. **Gaussian Elimination:**
for $t = T, T-1, \dots, 1$ # start furthest from root
 for $i \in L\{t\}$
 if $t > 1$
 $J \leftarrow N\{i\} \setminus L\{1 : t-1\}$ # neighbours that are not parent node
 if $J = \emptyset$ # i corresponds to a leaf node
 continue # no updates
 else
 $J \leftarrow N\{i\}$ # root node has no parent node
 $P_{Ji} \leftarrow \tilde{A}_{Ji}$ # initialize off-diagonal elements
 $P_{ii} \leftarrow P_{ii} - \sum_{j \in J} \frac{P_{ji}^2}{P_{jj}}$ # update diagonal elements of P in $L\{t\}$
 $C_i \leftarrow C_i - \sum_{j \in J} \frac{P_{ji}}{P_{jj}} \cdot C_j$

 3. **Backward Solve:**
for $t = 1, 2, \dots, T$ # start with root node
 for $i \in L\{t\}$
 if $t < T$
 $p \leftarrow N\{i\} \setminus L\{t+1 : T\}$ # parent node of i (empty for $t = 1$)
 else
 $p \leftarrow N\{i\}$ # only neighbour of leaf node is parent
 $x_i \leftarrow \frac{C_i - \tilde{A}_{ip} \cdot x_p}{P_{ii}}$ # solution to $\tilde{A}x = \tilde{c}$
-

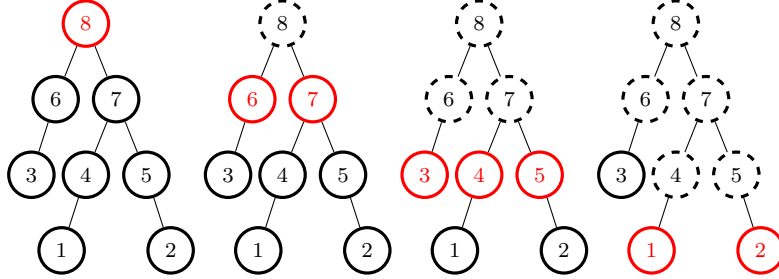


Figure 1: Process of partitioning nodes into level sets. For the above graph we have the following sets: $L\{1\} = \{8\}, L\{2\} = \{6, 7\}, L\{3\} = \{3, 4, 5\}$ and $L\{4\} = \{1, 2\}$.

size of $n/2$. We discuss how to generalize the red-black ordering to general graphs in the next section by using a greedy graph colouring algorithm, but we note that if the graph is very dense we may need a large of “colours” and our block sizes may be very small. Further, while red-black updating is highly-suitable for parallelization, its convergence rate may be slow as the update does not capture any dependencies between

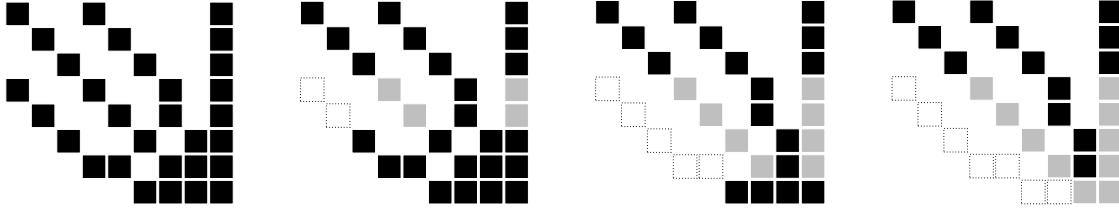


Figure 2: Illustration of Step 2 (row-reduction process) of Algorithm 1 for the tree in Figure 5. The matrix represents $[\tilde{A}|\tilde{c}]$. The black squares represent unchanged non-zero values of \tilde{A} and the grey squares represent non-zero values that are updated at some iteration in Step 2. In the final matrix (far right), the values in the last column are the values assigned to the vector C in Steps 1 and 2 above, while the remaining columns that form an upper triangular matrix are the values corresponding to the constructed P matrix. The backward solve of Step 3 solves the linear system.

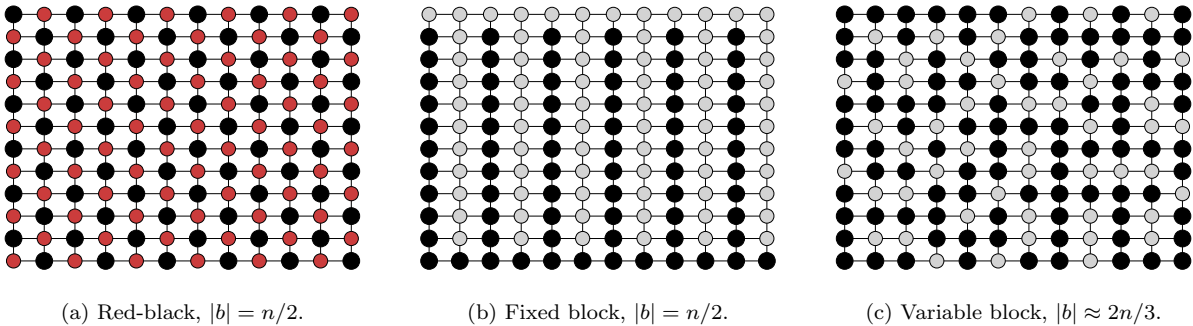


Figure 3: Partitioning strategies for defining forest-structured blocks.

the nodes of the same colour.

Diagonal matrices correspond to disconnected graphs, which are clearly forests (they have no edges). But message passing allows us to go beyond the red-black partitions, and update *any* forest-structured block in linear time. For example, the partition given in Figure 3b also has blocks of size $n/2$ but these blocks include dependencies. Our experiments indicate that such blocks make substantially more progress than using the red-black blocks or using smaller non-forest structured blocks. Further, we can extend these ideas to general graphs, where we could use any forest-structured partition of the nodes. However, the graph still does require some level of sparsity if we want larger block sizes as otherwise the forests may be very small (in the extreme case of a complete graph, forests can have at most 2 nodes).

Instead of fixed blocks, we can also consider forest-structured variable blocks. Here, instead of considering all blocks with cardinality τ as we have up to this point with variable blocks, we consider all blocks with a forest-structured induced subgraph. Thus, the block size may vary at each iteration but restricting to forests still leads to a linear-time update. As seen in Figure 3c, by allowing variable block sizes we can select a forest-structured block of size $|b| \approx 2n/3$ in one iteration (black nodes) while still maintaining a linear-time update. If we sample random forests, then the convergence rate under this strategy is covered by the arbitrary sampling theory [Qu et al., 2014]. Also note that the maximum of the gradient norms over all forests defines a valid norm, so our analysis of Gauss-Southwell can be applied to this case.

5.1 Partitioning into Forest-Structured Blocks

We can generalize the red-black approach to arbitrary graphs by defining our blocks such that no two neighbours are in the same block. While for lattice-structured graphs we only need two blocks to do this, for general graphs we may need a larger number of blocks. Finding the minimum number of blocks we need for a given graph is exactly the NP-hard graph colouring problem. Fortunately, there are various heuristics that quickly give a non-minimal valid colouring of the nodes. For example, in our experiments we used the following classic greedy algorithm [Welsh and Powell, 1967]:

1. Proceed through the vertices of the graph in some order $i = 1, 2, \dots, n$.
2. For each vertex i , assign it the smallest positive integer (“colour”) such that it doesn’t have the same colour as any of its neighbours among the vertices $\{1, 2, \dots, i - 1\}$.

We can use all vertices assigned to the same integer as our blocks in the algorithm, and if we apply this algorithm to a lattice-structured graph (using row- or column-ordering of the nodes) then we obtain the classic red-black colouring of the graph.

Instead of disconnected blocks, in this work we instead consider forest-structured blocks. The size of the largest possible forest is related to the graph colouring problem [Esperet et al., 2015], but we can consider a slight variation on the second step of the greedy colouring algorithm to find a set of forest-structured blocks:

1. Proceed through the vertices of the graph in some order $i = 1, 2, \dots, n$.
2. For each vertex i , assign it the smallest positive integer (“forest”) such that the nodes assigned to that integer among the set $\{1, 2, \dots, i\}$ form a forest.

If we apply this to a lattice structured graph (in column-ordering), this generates a partition into two forest-structured graphs similar to the one in Figure 3b (only the bottom row is different). This procedure requires us to be able to test whether adding a node to a forest maintains, and we show how to do this efficiently in Appendix D.

In the case of lattice-structured graph there is a natural ordering of the vertices, but for many graphs there is no natural ordering. In such we might simply consider a random ordering. Alternately, if we know the individual Lipschitz constants L_i , we could order by these values (with the largest L_i going first so that they are likely assigned to the same block if possible). In our experiments we found that this ordering improved performance for an unstructured dataset, and performed similarly to using the natural ordering in a lattice-structured dataset.

5.2 Approximate Greedy Rules with Forest-Structured Blocks

Similar to the problems of the previous section, computing the Gauss-Southwell rule over forest-structured variable blocks is NP-hard, as we can reduce the 3-satisfiability problem to the problem of finding a maximum-weight forest [Garey and Johnson, 1979]. However, we use a similar greedy method to approximate the greedy Gauss-Southwell rule over the set of trees:

1. Initialize b_k with the node i corresponding to the largest gradient, $|\nabla_i f(x^k)|$.
2. Search for the node i with the largest gradient that is not part of b_k and that maintains that b_k is a forest.
3. If such a node is found, add it to b_k and go back to step 2. Otherwise, stop.

Although this procedure does not yield the exact solution in general, it is appealing since (i) the procedure is efficient as it is easy to test whether adding a node maintains the forest property (see Appendix D), (ii) it outputs a forest so that the subsequent update is linear-time, (iii) we are guaranteed that the coordinate corresponding to the variable with the largest gradient is included in b_k , and (iv) we cannot add any additional node to the final forest and still maintain the forest property. A similar heuristic can be used to approximate the GSD rule under the restriction from Section 4.1 or to generate a forest randomly.

6 Manifold Identification

In this section we consider optimization problems of the form

$$\arg \min_{x \in \mathbb{R}^n} f(x) + \sum_{i=1}^n g_i(x_i), \quad (27)$$

where ∇f is Lipschitz-continuous and each g_i only needs to be convex and lower semi-continuous (it may be non-smooth or infinite at some x_i). A classic example of a problem in this framework is optimization subject to non-negative constraints,

$$\arg \min_{x \geq 0} f(x), \quad (28)$$

where in this case g_i is the indicator function on the non-negative orthant,

$$g_i(x_i) = \begin{cases} 0 & \text{if } x_i \geq 0, \\ \infty & \text{if } x_i < 0. \end{cases}$$

Another example that has received significant recent attention is the case of an L1-regularizer,

$$\arg \min_{x \in \mathbb{R}^n} f(x) + \lambda \|x\|_1, \quad (29)$$

where in this case $g_i = \lambda|x_i|$. Here, the L1-norm regularizer is used to encourage sparsity in the solution. A related problem is the group L1-regularization problem (6), where instead of being separable, g is block-separable.

Proximal gradient methods have become one of the default strategies for solving problem (27), and a BCD variant of these methods has an update of the form

$$x^{k+1} = \text{prox}_{\alpha_k g_{b_k}} [x^k - \alpha_k U_{b_k} \nabla_{b_k} f(x^k)], \quad (30)$$

where for any block b and step-size α the proximal operator is defined by the separable optimization

$$\text{prox}_{\alpha g_b}[x] = \arg \min_{y \in \mathbb{R}^n} \frac{1}{2\alpha} \|y - x\|^2 + \sum_{i \in b} g_i(y_i).$$

We note that all variables not in block b stay at their existing values in the optimal solution to this problem. In the special case of non-negative constraints like (28) the update in (30) is given by

$$x_i^{k+1} = \left[x_i - \frac{1}{L} \nabla_i f(x^k) \right]^+,$$

where $[\beta]^+ = \max\{0, \beta\}$ projects onto the non-negative orthant. For L1-regularization problems (29) the update reduces to an element-wise soft-thresholding step,

$$\begin{aligned} x_i^{k+\frac{1}{2}} &= x_i^k - \frac{1}{L} \nabla_i f(x^k), \\ x_i^{k+1} &= \frac{x_i^{k+\frac{1}{2}}}{|x_i^{k+\frac{1}{2}}|} \left[\left| x_i^{k+\frac{1}{2}} \right| - \frac{\lambda}{L} \right]^+, \end{aligned} \quad (31)$$

which we have written as a gradient update followed by the soft-threshold operator.

Most of the issues discussed in the previous sections for smooth BCD methods carry over in a straightforward way to this proximal setting; we can still consider fixed or variable blocks, there exist matrix and Newton updates, and we can still consider cyclic, random, or greedy selection rules. One subtle issue is

that there are many generalizations of the Gauss-Southwell rule to the proximal setting [Nutini et al., 2015]. However, the GS- q rule defined by Tseng and Yun [2009b] seems to be the generalization of GS with the best theoretical properties. A GSL variant of this rule would take the form

$$b_k \in \arg \min_{b \in \mathcal{B}} \left\{ \min_d \left\{ \langle \nabla_b f(x^k), d \rangle + \frac{L_b}{2} \|d\|^2 + \sum_{i \in b} g_i(x_i + d_i) - \sum_{i \in b} g_i(x_i) \right\} \right\}, \quad (32)$$

where we assume that the gradient of f is L_b -Lipschitz continuous with respect to block b . A generalization of the GS rule is obtained if we assume that the L_b are equal across all blocks.

It has been established that coordinate descent and BCD methods based on the update (30) for problem (27) obtain similar convergence rates to the case where we do not have a non-smooth term g [Nesterov, 2012, Nutini et al., 2015, Richtárik and Takáč, 2014]. The focus of this section is to show that *the non-smoothness of g can actually lead to a faster convergence rate*.

This idea dates back at least 40 years to the work of Bertsekas [1976]¹¹. For the case of non-negative constraints, he shows that the sparsity pattern of x^k generated by the projected-gradient method matches the sparsity pattern of the solution x^* for all sufficiently large k . Thus, after a finite number of iterations the projected-gradient method will “identify” the final set of non-zero variables. Once these values are identified, Bertsekas suggests that we can fix the zero-valued variables and apply an unconstrained Newton update to the set of non-zero variables to obtain superlinear convergence. Even without switching to a superlinearly-convergent method, the convergence rate of the projected-gradient method can be faster once the set of non-zeroes is identified since it is effectively optimizing in the lower-dimensional space corresponding to the non-zero variables.

This idea of identifying a smooth “manifold” containing the solution x^* has been generalized to allow polyhedral constraints [Burke and Moré, 1988], general convex constraints [Wright, 1993], and even non-convex constraints [Hare and Lewis, 2004]. Similar results exist in the proximal gradient setting. For example, it has been shown that the proximal gradient method identifies the sparsity pattern in the solution of L1-regularized problems after a finite number of iterations [Hare, 2011]. The active-set identification property has also been shown for other algorithms like certain coordinate descent and stochastic gradient methods [Lee and Wright, 2012, Mifflin and Sagastizábal, 2002, Wright, 2012]. Specifically, Wright shows that BCD also has this manifold identification property for separable g [Wright, 2012], provided that the coordinates are chosen in an essentially-cyclic way (or provided that we can simultaneously choose to update all variables that do not lie on the manifold). Wright also shows that superlinear convergence is possible if we use a Newton update on the manifold, assuming the Newton update does not leave the manifold.

In the next subsection, we present a manifold identification result for proximal coordinate descent for general separable g . We follow a similar argument to Bertsekas [1976], which yields a simple proof that holds for many possible selection rules including greedy rules (which may not be essentially-cyclic). Further, our argument leads to bounds on the *active-set complexity* of the method, which is the number of iterations required to reach the manifold [Nutini et al., 2017]. As examples, we consider problems (28) and (29), and show explicit bounds for the active-set complexity. We subsequently show how to generalize this argument to cases like block updates and Newton updates. The latter naturally leads to superlinear convergence of greedy BCD methods when using variable blocks of size larger than the dimension of the manifold.

6.1 Manifold Identification for Separable g

Assume the subdifferential of g is nonempty for all $x \in \text{dom}(g)$. By our separability assumption on g , the subdifferential of g can be expressed as the concatenation of the individual subdifferential of each g_i , where the subdifferential of g_i at any $x_i \in \mathbb{R}$ is defined by

$$\partial g_i(x_i) = \{v \in \mathbb{R} : g_i(y) \geq g_i(x_i) + v \cdot (y - x_i), \text{ for all } y \in \text{dom}(g_i)\}.$$

¹¹A similar property was shown for proximal point methods in a more general setting around the same time, [Rockafellar, 1976].

This implies that the subdifferential of each g_i is just an interval on the real line. In particular, the interior of the subdifferential of each g_i at a non-differentiable point x_i can be written as an open interval,

$$\text{int } \partial g_i(x_i) \equiv (l_i, u_i), \quad (33)$$

where $l_i \in \mathbb{R} \cup \{-\infty\}$ and $u_i \in \mathbb{R} \cup \{\infty\}$ (the ∞ values occur if x_i is at its lower or upper bound, respectively). The *active-set* at a solution x^* for a separable g is then defined by

$$\mathcal{Z} = \{i : \partial g_i(x_i^*) \text{ is not a singleton}\}.$$

By (33), the set \mathcal{Z} includes indices i where x_i^* is equal to the lower bound on x_i , is equal to the upper bound on x_i , or occurs at a non-smooth value of g_i . In our examples of non-negative constraints or L1-regularization, \mathcal{Z} is the set of coordinates that are zero at the solution x^* . With this definition, we can formally define the manifold identification property.

Definition 1. *The manifold identification property for problem (27) is satisfied if for all sufficiently large k , we have that $x_i^k = x_i^*$ for some solution x^* for all $i \in \mathcal{Z}$.*

In order to prove the manifold identification property for the proximal coordinate descent method, in addition to assuming that ∇f is L -Lipschitz continuous, we require two assumptions. Our first assumption is that the iterates of the algorithm converge to a solution x^* .

Assumption 1. *The iterates of the proximal coordinate descent method converge to an optimal solution x^* of problem (27), that is $x^k \rightarrow x^*$ as $k \rightarrow \infty$.*

This assumption holds if f is strongly-convex and if we use cyclic or greedy selection (see Appendix E), but will also hold under a variety of other scenarios. Our second assumption is a *nondegeneracy* condition on the solution x^* that the algorithm converges to. Below we write the standard nondegeneracy condition from the literature for our special of (27).

Assumption 2. *We say that x^* is a nondegenerate solution for problem (27) if it holds that*

$$\begin{cases} -\nabla_i f(x^*) = \nabla_i g(x_i^*) & \text{if } \partial g_i(x_i^*) \text{ is a singleton (} g_i \text{ is smooth at } x_i^*) \\ -\nabla_i f(x^*) \in \text{int } \partial g_i(x_i^*) & \text{if } \partial g_i(x_i^*) \text{ is not a singleton (} g_i \text{ is non-smooth at } x_i^*). \end{cases}$$

This condition states that $-\nabla f(x^*)$ must be in the “relative interior” (see [Boyd and Vandenberghe, 2004, Section 2.1.3]) of the subdifferential of g at the solution x^* . In the case of the non-negative bound constrained problem (28), this requires that $\nabla_i f(x^*) > 0$ for all variables i that are zero at the solution ($x_i^* = 0$). For the L1-regularization problem (29), this requires that $|\nabla_i f(x^*)| < \lambda$ for all variables i that are zero at the solution.¹²

There are three results that we require in order to prove the manifold identification property. The first result follows directly from Assumption 1 and establishes that for any $\beta > 0$ there exists a finite iteration \bar{k} such that the distance from the iterate x^k to the solution x^* for all iterations $k \geq \bar{k}$ is bounded above by β .

Lemma 1. *Let Assumption 1 hold. For any β , there exists some minimum finite \bar{k} such that $\|x^k - x^*\| \leq \beta$ for all $k \geq \bar{k}$.*

The second result we require is that for any $i \in \mathcal{Z}$ such that $x_i^k \neq x_i^*$, eventually coordinate i is selected at some finite iteration.

Lemma 2. *Let Assumption 1 hold. If $x_i^k \neq x_i^*$ for some $i \in \mathcal{Z}$, then coordinate i will be selected by the proximal coordinate descent method after a finite number of iterations.*

¹²Note that $|\nabla_i f(x^*)| \leq \lambda$ for all i with $x_i^* = 0$ follows from the optimality conditions, so this assumption simply rules out the case where $|\nabla_i f(x_i^*)| = \lambda$. We note that in this case the nondegeneracy condition is a strict complementarity condition [De Santis et al., 2016].

Proof. For eventual contradiction, suppose we did not select such an i after iteration k' . Then for all $k \geq k'$ we have that

$$|x_i^{k'} - x_i^*| = |x_i^k - x_i^*| \leq \|x^k - x^*\|. \quad (34)$$

By Assumption 1 the right-hand side is converging to 0, so it will eventually be less than $|x_i^{k'} - x_i^*|$ for some $k \geq k'$, contradicting the inequality. Thus after a finite number of iterations we must have that $x_i^k \neq x_i^{k'}$, which can only be achieved by selecting i . \square

The third result we require is that once Lemma 1 is satisfied for some finite \bar{k} and a particular $\beta > 0$, then for any coordinate $i \in \mathcal{Z}$ selected at some iteration $k' \geq \bar{k}$ by the proximal coordinate descent method, we have $x_i^{k'} = x_i^*$. We prove that this happens for a value β depending on a quantity δ defined by

$$\delta = \min_{i \in \mathcal{Z}} \{ \min \{ -\nabla_i f(x^*) - l_i, u_i + \nabla_i f(x^*) \} \}, \quad (35)$$

which is the minimum distance to the nearest boundary of the subdifferential (33) among indices $i \in \mathcal{Z}$.

Lemma 3. *Consider problem (27), where f is convex with L -Lipschitz continuous gradient and the g_i are proper convex functions (not necessarily smooth). Let Assumptions 1 be satisfied and Assumption 2 be satisfied for the particular x^* that the algorithm converges to. Then for any proximal coordinate descent method with a step-size of $1/L$, if $\|x^k - x^*\| \leq \delta/2L$ holds and $i \in \mathcal{Z}$ is selected at iteration k , then $x_i^{k+1} = x_i^*$.*

Proof. The proof is identical to the case of proximal-gradient updates under the same step-size [Nutini et al., 2017, Lemma 1], but restricting to the update of the single coordinate. \square

With the above results we next have the manifold identification property.

Theorem 3. *Consider problem (27), where f is convex with L -Lipschitz continuous gradient and the g_i are proper convex functions. Let Assumptions 1 be satisfied and Assumption 2 be satisfied for the particular x^* that the algorithm converges to. Then for any proximal coordinate descent method with a step-size of $1/L$ there exists a finite k such that $x_i^k = x_i^*$ for all $i \in \mathcal{Z}$.*

Proof. Lemma 1 implies that the assumptions of Lemma 3 are eventually satisfied, and combining this with Lemma 2 we have our result. \square

Both problems (28) and (29) satisfy the manifold identification result. By the definition of δ in (35), we have that $\delta = \min_{i \in \mathcal{Z}} \{ \nabla_i f(x^*) \}$ for problem (28). We note that if $\delta = 0$, then we may approach the manifold through the interior of the domain and the manifold may never be identified (this is the purpose of the nondegeneracy condition). For problem (29), we have that $\delta = \lambda - \max_{i \in \mathcal{Z}} \{ |\nabla_i f(x^*)| \}$ for problem (29). From these results, we are able to define explicit bounds on the number of iterations required to reach the manifold, a new result that we explore in the next subsection.

Instead of using a step-size of $1/L$, it is more common to use a bigger step-size of $1/L_i$ within coordinate descent methods, where L_i is the coordinate-wise Lipschitz constant. In this case, the results of Lemma 3 hold for $\beta = \delta/(L + L_i)$. This is a larger region since $L_i \leq L$, so with this standard step-size the iterates can move onto the manifold from further away and we expect to identify the manifold earlier. The argument can also be modified to use other step-size selection methods, provided that we can write the algorithm in terms of a step-size α_k that is guaranteed to be bounded from below. While the above result considers single-coordinate updates, it can trivially be modified to show that BCD with gradient updates has the manifold identification property. The only change is that once $\|x^k - x^*\| \leq \delta/2L$, we have that $x_i^{k+1} = x_i^*$ for all $i \in b_k \cap \mathcal{Z}$. Thus, BCD methods can simultaneously move many variables onto the optimal manifold.

6.2 Active-Set Complexity

The manifold identification property of the previous section could also be shown using the more sophisticated tools used in related works [Burke and Moré, 1988, Hare and Lewis, 2004]. However, an appealing aspect of the simple argument is that it can be combined with non-asymptotic convergence rates of the iterates to bound the *number of iterations required to reach the manifold*. We call this the “active-set complexity” of the method, and have recently given bounds on the active-set complexity of proximal-gradient methods for strongly-convex objectives [Nutini et al., 2017]. Here we use a similar analysis to bound the active-set complexity of BCD methods, which is complicated by the fact that not all coordinates are updated on each iteration.

We will consider the active-set complexity in the case where f is strongly-convex and we use cyclic or greedy selection. This guarantees that

$$\|x^k - x^*\| \leq \left(1 - \frac{1}{\kappa}\right)^k \gamma, \tag{36}$$

for some $\gamma \geq 0$ and some $\kappa \geq 1$ (see Appendix E, and we note that this type of rate also holds for a variety of other types of selection rules). By using that $(1 - 1/\kappa)^k \leq \exp(-k/\kappa)$, the linear convergence rate (36) implies the following result on how many iterations it will take to identify the active-set, and thus reach the manifold.

Theorem 4. *Consider any method that achieves an iterate bound (36). For δ as defined in (35), we have $\|x^{\bar{k}} - x^*\| \leq \delta/2L$ after at most $\kappa \log(2L\gamma/\delta)$ iterations. Further, we will identify the active-set after an additional t iterations, where t is the number of additional iterations required to select all suboptimal x_i with $i \in \mathcal{Z}$ as part of some block.*

The value of t depends on the selection rule we use. If we use cyclic selection we will require at most $t = n$ additional iterations to select all suboptimal coordinates $i \in \mathcal{Z}$ and thus to reach the optimal manifold. To bound the active-set complexity for general rules like greedy rules, we cannot guarantee that all coordinates will be selected after n iterations once we are close to the solution. In the case of non-negative constraints, the number of additional iterations depends on a quantity we will call ϵ , which is the smallest non-zero variable $x_i^{\bar{k}}$ for $i \in \mathcal{Z}$ and \bar{k} satisfying the first part of Theorem 4. It follows from (36) that we require at most $\kappa \log(\gamma/\epsilon)$ iterations beyond \bar{k} to select all non-zero $i \in \mathcal{Z}$. Thus, the active-set complexity for greedy rules for problem (28) is bounded above by $\kappa(\log(2L\gamma/\delta) + \log(\gamma/\epsilon))$. Based on this bound, greedy rules (which yield a smaller κ) may identify the manifold more quickly than cyclic rules in cases where ϵ is large. However, if ϵ is very small then greedy rules may take a larger number of iterations to reach the manifold.¹³

6.3 Proximal-Newton Updates and Superlinear Convergence

Once we have identified the optimal manifold, we can think about switching from using the proximal BCD method to using an unconstrained optimizer on the coordinates $i \notin \mathcal{Z}$. The unconstrained optimizer can be a Newton update, and thus under the appropriate conditions can achieve superlinear convergence. However, a problem with such “2-phase” approaches is that we do not know the exact time at which we reach the optimal manifold. This can make the approach inefficient: if we start the second phase too early, then we sub-optimize over the wrong manifold, while if we start the second phase too late, then we waste iterations performing first-order updates when we should be using second-order updates. Wright proposes an interesting alternative where at each iteration we consider replacing the gradient proximal-BCD update with a Newton update on the current manifold [Wright, 2012]. This has the advantage that the manifold can continue to be updated, and that Newton updates are possible as soon as the optimal manifold has been identified. However, note that the dimension of the current manifold might be larger than the block size and the dimension of the optimal manifold, so this approach can significantly increase the iteration cost for some problems.

¹³If this is a concern, the implementer could consider a safeguard ensuring that the method is essentially-cyclic. Alternately, we could consider rules that prefer to include variables that are near the manifold and have the appropriate gradient sign.

Rather than “switching” to an unconstrained Newton update, we can alternately take advantage of the superlinear converge of proximal-Newton updates [Lee et al., 2012]. For example, in this section we consider Newton proximal-BCD updates as in several recent works [Fountoulakis and Tappenden, 2015, Qu et al., 2016, Tappenden et al., 2016]. For a block b these updates have the form

$$x_b^{k+1} \in \arg \min_{y \in \mathbb{R}^{|b|}} \left\{ \langle \nabla_b f(x_b^k), y - x_b^k \rangle + \frac{1}{2\alpha_k} \|y - x_b^k\|_{H_b^k}^2 + \sum_{i \in b} g_i(y_i) \right\}, \quad (37)$$

where H_b^k is the matrix corresponding to block b at iteration k (which can be the sub-Hessian $\nabla_{bb}^2 f(x^k)$). As before if we set $H_b^k = H_b$ for some fixed matrix H_b , then we can take $\alpha_k = 1$ if block b of f is 1-Lipschitz continuous in the H_b -norm.

In the next section, we give a practical variant on proximal-Newton updates that also has the manifold identification property under standard assumptions¹⁴. An advantage of this approach is that the block size typically restricts the computational complexity of the Newton update (which we discuss further in the next sections). Further, superlinear convergence is possible in the scenario where the coordinates $i \notin \mathcal{Z}$ are chosen as part of the block b_k for all sufficiently large k . However, note that this superlinear scenario only occurs in the special case where we use a *greedy rule with variable blocks* and where the *size of the blocks is at least as large as the dimension of the optimal manifold*. With variable blocks, the GS- q and GSL- q rules (32) will no longer select coordinates $i \in \mathcal{Z}$ since their optimal d_i value is zero when close to the solution and on the manifold. Thus, these rules will only select $i \notin \mathcal{Z}$ once the manifold has been identified.¹⁵ In contrast, we would not expect superlinear convergence for fixed blocks unless all $i \notin \mathcal{Z}$ happen to be in the same partition. While we could show superlinear convergence of subsequences for random selection with variable blocks, the number of iterations between elements of the subsequence may be prohibitively large.

6.4 Practical Proximal-Newton Methods

A challenge with using the update (37) in general is that the optimization is non-quadratic (due to the g_i terms) and non-separable (due to the H_b^k -norm). If we make the H_b^k diagonal, then the objective is separable but this destroys the potential for superlinear convergence. Fortunately, a variety of strategies exist in the literature to allow non-diagonal H_b^k .

For example, for bound constrained problems we can apply two-metric projection (TMP) methods, which use a modified H_b^k and allow the computation of a (cheap) projection under the Euclidean norm [Gafni and Bertsekas, 1984]. This method splits the coordinates into an “active-” set and a “working-” set, where the active-set \mathcal{A} for non-negative constraints would be

$$\mathcal{A} = \{i \mid x_i < \epsilon, \nabla_i f(x) > 0\},$$

for some small ϵ while the working-set \mathcal{W} is the compliment of this set. So the active-set contains the coordinates corresponding to the variables that we expect to be zero while the working-set contains the coordinates corresponding to the variables that we expect to be unconstrained. The TMP method can subsequently use the update

$$\begin{aligned} x_{\mathcal{W}} &\leftarrow \text{proj}_C(x_{\mathcal{W}} - \alpha H_{\mathcal{W}}^{-1} \nabla_{\mathcal{W}} f(x)) \\ x_{\mathcal{A}} &\leftarrow \text{proj}_C(x_{\mathcal{A}} - \alpha \nabla_{\mathcal{A}} f(x)). \end{aligned}$$

This method performs a gradient update on the active-set and a Newton update on the working-set. Gafni and Bertsekas [1984] show that this preserves many of the essential properties of projected-Newton methods

¹⁴A common variation of the proximal-Newton method solves (37) with $\alpha_k = 1$ and then sets x^{k+1} based on a search along the line segment between x^k and this solution [Fountoulakis and Tappenden, 2015, Schmidt, 2010]. This variation does *not* have the manifold identification property; only when the line search is on α_k do we have this property.

¹⁵A subtle issue is the case where $d_i = 0$ in (32) but $i \notin \mathcal{Z}$. In such cases we can break ties by preferring coordinates i , where g_i is differentiable so that the $i \notin \mathcal{Z}$ are included.

like giving a descent direction, converging to a stationary point, and superlinear convergence if we identify the correct set of non-zero variables. Also note that for indices $i \in \mathcal{Z}$, this eventually only takes gradient steps so our analysis of the previous section applies (it identifies the manifold in a finite number of iterations). As opposed to solving the block-wise proximal-Newton update in (37), in our experiments we explored simply using the TMP update applied to the block and found that it gave nearly identical performance.

TMP methods have also been generalized to settings like L1-regularization [Schmidt, 2010] and they can essentially be used for any separable g function. Another widely-used strategy is to inexactly solve (37) [Fountoulakis and Tappenden, 2015, Lee et al., 2012, Schmidt, 2010]. This has the advantage that it can still be used in the group L1-regularization setting or other group-separable settings.

6.5 Optimal Updates for Quadratic f and Piecewise-Linear g

Two of the most well-studied optimization problems in machine learning are the SVM and LASSO problems. The LASSO problem is given by an L1-regularized quadratic objective

$$\arg \min_x \frac{1}{2} \|Ax - b\|^2 + \lambda \|x\|_1,$$

while the dual of the (non-smooth) SVM problem has the form of a bound-constrained quadratic objective

$$\arg \min_{0 \leq x \leq \gamma} \frac{1}{2} x^T A x,$$

for some matrix A (positive semi-definite in the SVM case), and regularization constants λ and γ . In both cases we typically expect the solution to be sparse, and identifying the optimal manifold has been shown to improve practical performance of BCD methods [De Santis et al., 2016, Joachims, 1999].

Both problems have a set of g_i that are piecewise-linear over their domain, implying that they can be written as a maximum over univariate linear functions on the domain of each variable. Although we can still consider TMP or inexact proximal-Newton updates for these problems, this special structure actually allows us to compute the exact minimum with respect to a block (which is efficient when considering medium-sized blocks). Indeed, for SVM problems the idea of using exact updates in BCD methods dates back to the sequential minimal optimization (SMO) method [Platt, 1998], which uses exact updates for blocks of size 2. In this section we consider methods that work for blocks of arbitrary size.¹⁶

While we could write the optimal update as a quadratic program, the special structure of the LASSO and SVM problems lends well to exact homotopy methods. These methods date back to Osborne and Turlach [2011], Osborne et al. [2000] who proposed an exact homotopy method that solves the LASSO problem for all values of λ . This type of approach was later popularized under the name “least angle regression” (LARS) [Efron et al., 2004]. Since the solution path is piecewise-linear, given the output of a homotopy algorithm we can extract the exact solution for our given value of λ . Hastie et al. [2004] derive an analogous homotopy method for SVMs, while Rosset and Zhu [2007] derive a generic homotopy method for the case of piecewise-linear g_i functions.

The cost of each iteration of a homotopy method on a problem with $|b|$ variables is $O(|b|^2)$. It is known that the worst-case runtime of these homotopy methods can be exponential [Mairal and Yu, 2012]. However, the problems where this arises are somewhat unstable, and in practice the solution is typically obtained after a linear number of iterations. This gives a runtime in practice of $O(|b|^3)$, which does not allow enormous blocks but does allow us to efficiently use block sizes in the hundreds or thousands. That being said, since these methods compute the exact block update, in the scenario where we previously had superlinear convergence, we now obtain *finite* convergence. That is, the algorithm will stop in a finite number of iterations with the exact solution *provided that* it has identified the optimal manifold, uses a greedy rule with variable blocks, and the block size is larger than the dimension of the manifold. This finite termination is also guaranteed under similar assumptions for TMP methods, and although TMP methods may make less

¹⁶The methods discussed in this section can also be used to compute exact Newton-like updates in the case of a non-quadratic f , but where the g_i are still piecewise-linear.

progress per-iteration than exact updates, they may be a cheaper alternative to homotopy methods as the cost is explicitly restricted to $O(|b|^3)$.

7 Numerical Experiments

We performed an extensive variety of experiments to evaluate the effects of the contributions listed in the previous sections. In this section we include several of these results that highlight some key trends we observed, and in each subsection below we explicitly list the insights we obtained from the experiment. We considered five datasets that evaluate the methods in a variety of scenarios:

- A Least-squares with a sparse data matrix.
- B Binary logistic regression with a sparse data matrix.
- C 50-class logistic regression problem with a sparse data matrix.
- D Lattice-structured quadratic objective as in Section 5.
- E Binary label propagation problem (sparse but unstructured quadratic).

For interested readers, we give the full details of these datasets in Appendix F where we have also included our full set of experiment results.

In our experiments we use the number of iterations as our measure of performance. This measure is far from perfect, especially when considering greedy methods, since it ignores the computational cost of each iteration. But this measure of performance provides an implementation- and problem-independent measure of performance. We seek an implementation-independent measure of performance since the actual runtimes of different methods will vary wildly across applications. However, it is typically easy to estimate the per-iteration runtime when considering a new problem. Thus, we hope that our quantification of what can be gained from more-expensive methods gives guidance to readers about whether the more-expensive methods will lead to a performance gain on their applications. In any case, we are careful to qualify all of our claims with warnings in cases where the iteration costs differ.

7.1 Greedy Rules with Gradient Updates

Our first experiment considers gradient updates with a step-size of $1/L_b$, and seeks to quantify the effect of using fixed blocks compared to variable blocks (Section 3.1) as well as the effect of using the new GSL rule (Section 3.2). In particular, we compare selecting the block using Cyclic, Random, Lipschitz (sampling the elements of the block proportional to L_i), GS, and GSL rules. For each of these rules we implemented a fixed block (FB) and variable block (VB) variant. For VB using Cyclic selection, we split a random permutation of the coordinates into equal-sized blocks and updated these blocks in order (followed by using another random permutation). To approximate the seemingly-intractable GSL rule with VB, we used the GSD rule (Section 3.4) using the SIRT-style approximation (23) from Section 4.1. We used the bounds in Appendix B to set the L_b values. To construct the partition of the coordinates needed in the FB method, we sorted the coordinates according to their L_i values then placed the largest L_i values into the first block, the next set of largest in the second block, and so on.

We plot selected results in Figure 4, while experiments on all datasets and with other block sizes are given in Appendix F.2. Overall, we observed the following trends:

- **Greedy rules tend to outperform random and cyclic rules**, particularly with small block sizes. This difference is sometimes enormous, and this suggests we should prefer greedy rules when the greedy rules can be implemented with a similar cost to cyclic or random selection.
- **The variance of the performance between the rules becomes smaller as the block size increases.** This is because the performance of all methods increases with the block size, and suggests

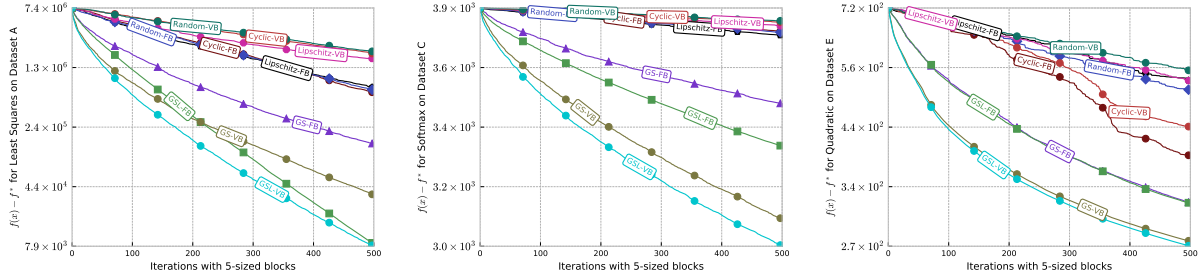


Figure 4: Comparison of different random and greedy block selection rules on three different problems when using gradient updates.

that if we use very-large block sizes with gradient updates that we should prefer simple Cyclic or Random updates.

- **VB can substantially outperform FB when using GS** for certain problems. This is because FB are a subset of the VB, so we can make the progress bound better. Thus, we should prefer GS-VB for problems where this has a similar cost to GS-FB. We found *this trend was reversed for random rules*, where fixed blocks tended to perform better. We suspect this trend is due to the coupon collector problem: it takes FB fewer iterations than VB to select all variables at least once given that the sample size for FB is smaller.
- **GSL consistently improved on the classic GS rule**, and in some cases the new rule with FB even outperformed the GS rule with VB. Interestingly, the performance gain was larger in the block case than in the prior work looking at the single-coordinate case [Nutini et al., 2015].

In Appendix F we repeat this experiment for the FB methods but using the approximation to L_b discussed in Section 4.3 (see Figures 9). This sought to test whether this procedure, which may underestimate the true L_b and thus use larger step-sizes, would improve performance. This experiment lead to some additional insights:

- **Approximating L_b was more effective as the block size increases.** This makes sense, since with large block sizes there are more possible directions and we are unlikely to ever need to use a step-size as small as $1/L_b$ for the global L_b .
- **Approximating L_b is far more effective than using a loose bound.** We have relatively-good bounds for all problems except Problem C. On this problem the Lipschitz approximation procedure was much more effective even for small block sizes.

This experiment suggests that we should prefer to use an approximation to L_b (or an explicit line-search) when using gradient updates unless we have a tight approximation to the true L_b and we are using a small block size. We also performed experiments with different block partitioning strategies for FB (see Figure 10). Although these experiments had some variability, we found that the block partitioning strategy did not make a large difference for cyclic and random rules. In contrast, when using greedy rules our sorting approach tended to outperform using random blocks or choosing the blocks to have similar average Lipschitz constants.

7.2 Greedy Rules with Matrix Updates

Our next experiment considers using matrix updates based on the matrices H_b from Appendix B, and quantifies the effects of the GSQ and GSD rules introduced in Sections 3.3-3.4 as well the approximations to these introduced in Sections 4.1-4.2. In particular, for FB we consider the GS rule and the GSL rule (from

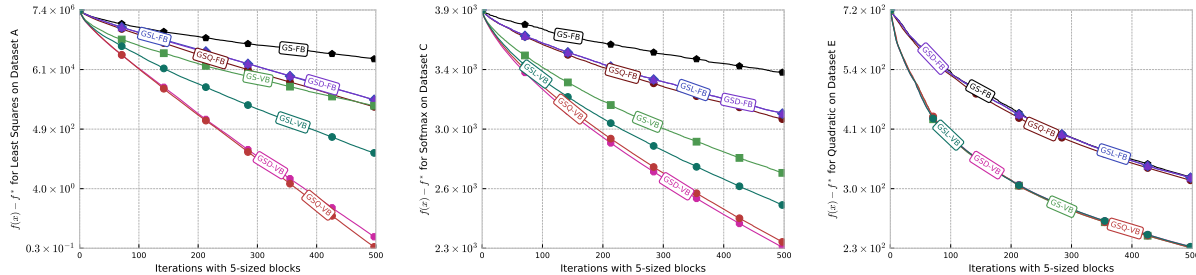


Figure 5: Comparison of different greedy block selection rules on three different problems when using matrix updates.

the previous experiment), the GSD rule (using the diagonal matrices from Section 4.1 with $D_{b,i} = L_i$), and the GSQ rule (which is optimal for the three quadratic objectives). For VB we consider the GS rule from the previous experiment as well as the GSD rule (using $D_{b,i} = L_i$), and the GSQ rule using the approximation from Section 4.2 and 10 iterations of iterative hard thresholding. Other than switching to matrix updates and focusing on these greedy rules, we keep all other experimental factors the same.

We plot selected results of doing this experiment in Figure 5. These experiments showed the following interesting trends:

- **There is a larger advantage to VB with matrix updates.** When using matrix updates, the basic GS-VB method outperformed even the most effective GSQ-FB rule for smaller block sizes.
- **There is little advantage to GSD/GSQ with FB.** Although the GSL rule consistently improved over the classic GS rule, we did not see any advantage to using the more-advanced GSD or GSQ rules when using FB.
- **GSD outperformed GS with VB.** Despite the use of a crude approximation to the GSD rule, the GSD rule consistently outperformed the classic GS rule. The GSD-VB method (which uses $D_i = L_i$) consistently outperformed the GSL-VB method (which uses a different diagonal scaling with a tighter bound), despite the GSL-VB having better performance when using gradient updates.
- **GSQ slightly outperformed GSD with VB and large blocks.** Although the GSQ-VB rule performed the best across all experiments, the difference was more noticeable for large block sizes. However, this did not offset its high cost in any experiment. We also experimented with OMP instead of IHT, and found it gave a small improvement but the iterations were substantially more expensive.

Putting the above together, with matrix updates our experiments indicate that the GSD rule seems to both provide good performance in all settings. We would only recommend using the GSQ rule in settings where we can use VB and where operations involving the objective f are much more expensive than running an IHT or OMP method. We performed experiments with different block partition strategies for FB, but found that when using matrix updates the partitioning strategy did not make a big difference for cyclic, random, or greedy rules.

In Appendix F we repeat this experiment for the non-quadratic objectives using the Newton direction and a backtracking line-search to set the step-size (see Figure 12), as discussed in Sections 4.4 and 4.6. For both datasets, the Newton updates resulted in a significant performance improvement over the matrix updates. This indicates that we should prefer classic Newton updates over the more recent matrix updates for non-quadratic objectives where computing the sub-block of the Hessian is tractable.

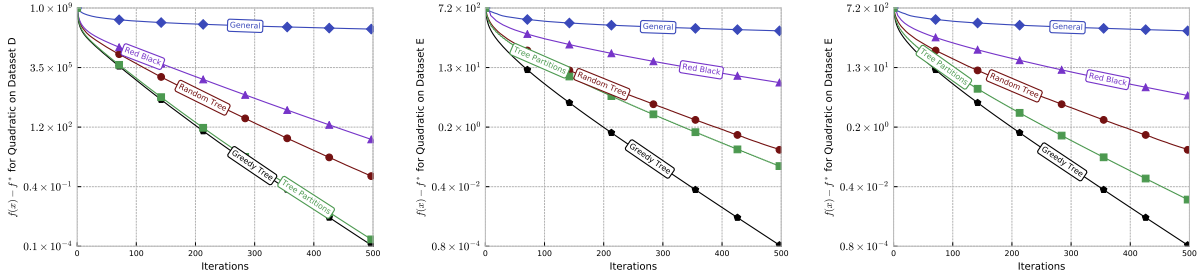


Figure 6: Comparison of different greedy block selection rules on two quadratic graph-structured problems when using optimal updates. The middle figure considers a random ordering for the Red Black and Tree Partition methods, while the right figure sorts by the Lipschitz constants for these methods.

7.3 Message-Passing Updates

We next seek to quantify the effect of using message-passing to efficiently implement exact updates for quadratic functions, as discussed in Section 5. For this experiment, we focused on the lattice-structured dataset D and the unstructured but sparse dataset E. These are both quadratic objectives with high treewidth, but that allow us to find large forest-structured induced subgraphs. We compared the following strategies to choose the block: greedily choosing the best general unstructured blocks using GS (General), cycling between blocks generated by the greedy graph colouring algorithm of Section 5.1 (Red Black), cycling between blocks generated by the greedy forest-partitioning algorithm of Section 5.1 (Tree Partitions), greedily choosing a tree using the algorithm of Section 5.2 (Greedy Tree), and growing a tree randomly using the same algorithm (Random Tree). For the lattice-structured Dataset D, the greedy partitioning algorithms proceed through the variables in order which generate partitions similar to those shown in in Figure 3b. For the unstructured Dataset E, we apply the greedy partitioning strategies of Section 5.1 using both a random ordering and by sorting the Lipschitz constants L_i . Since the cost of the exact update for tree-structured methods is $O(n)$, for the unstructured blocks we chose a block size of $b_k = n^{1/3}$ to make the costs comparable (since the exact solve is cubic in the block size for unstructured blocks).

We plot selected results of doing this experiment in Figure 6. Here, we see that even the classic red-black ordering outperforms using general unstructured blocks (since we must use such small block sizes). The tree-structured blocks perform even better, and in the unstructured setting our greedy approximation of the GS rule under variable blocks outperforms the other strategies. However, our greedy tree partitioning method also performs well. For the lattice-structured data it performed similarly to the greedy approximation, while for the unstructured data it outperformed all methods except greedy (and performed better when sorting by the Lipschitz constants than using a random order).

7.4 Proximal Updates

Our final experiment demonstrates the manifold identification and superlinear/finite convergence properties of the greedy BCD method as discussed in Section 6 for a sparse non-negative constrained L1-regularized least-squares problem using Dataset A. In particular, we compare the performance of a projected gradient update with L_b step-size, a projected Newton (PN) solver with line search as discussed in Section 6.3 and the two-metric projection (TMP) update as discussed in Section 6.4 when using fixed (FB) and variable (VB) blocks of different sizes ($|b| \in \{5, 50, 100\}$). We use a regularization constant of $\lambda = 50,000$ to encourage a high level of sparsity resulting in an optimal solution x^* with 51 non-zero variables. In Figure 7 we indicate active-set identification with a star and show that all approaches eventually identify the active-set. We see that TMP does as well as projected Newton for all block sizes and both do better than gradient updates. For a block size of 100, we get finite convergence using projected Newton and TMP updates.

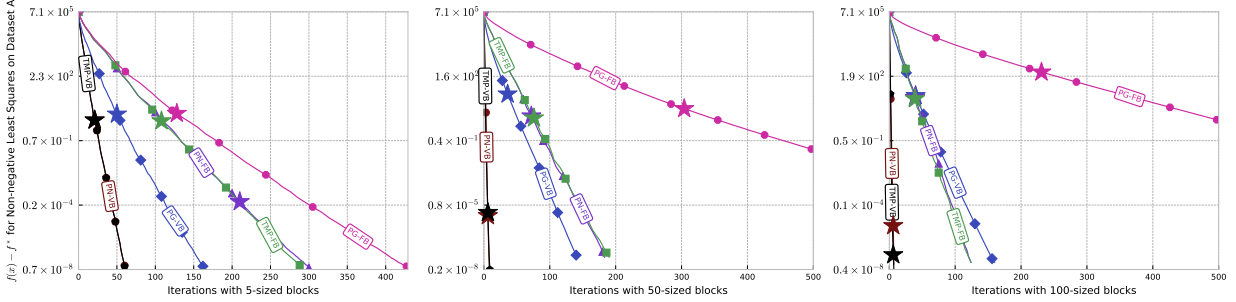


Figure 7: Comparison of different updates when using greedy fixed and variable blocks of different sizes.

In Appendix F.4 we repeat this experiment for random block selection and show that for such a sparse problem multiple iterations are often required before progress is made due to the repetitive selection of variables that are already zero/active.

8 Discussion

In this work we focused on non-accelerated BCD methods. However, we expect that our conclusions are likely to also apply for accelerated BCD methods [Fercoq and Richtárik, 2015]. Similarly, while we focused on the setting of serial computation, we expect that our conclusions will give insight into developing more efficient parallel and distributed BCD methods [Richtárik and Takáč, 2016].

Although our experiments indicate that our choice of the diagonal matrices D within the GSD rule provides a consistent improvement, this choice is clearly sub-optimal. A future direction is to find a generic strategy to construct better diagonal matrices, and work on ESO methods could potentially be adapted for doing this [Qu and Richtárik, 2016]. This could be in the setting where we are given knowledge of the Lipschitz constants, but a more-interesting idea is to construct these matrices online as the algorithm runs.

The GSQ rule can be viewed as a greedy rule that incorporates more sophisticated second-order information than the simpler GS and GSL rules. In preliminary experiments, we also considered selection rules based on the cubic regularization bound. However, these did not seem to converge more quickly than the existing rules in our experiments, and it is not obvious how one could efficiently implement such second-order rules.

We focused on BCD methods that approximate the objective function at each step by globally bounding higher-order terms in a Taylor expansion. However, we would expect more progress if we could bound these locally in a suitably-larger neighbourhood of the current iteration. Alternately, note that bounding the Taylor expansion is not the only way to upper bound a function. For example, Khan [2012] discusses a variety of strategies for bounding the binary logistic regression loss and indeed proves that other bounds are tighter than the Taylor expansion (“Bohning”) bound that we use. It would be interesting to explore the convergence properties of BCD methods whose bounds do not come from a Taylor expansion.

While we focused on the case of trees, there are message-passing algorithms that allow graphs with cycles [Rose, 1970, Srinivasan and Todorov, 2015]. The efficiency of these methods depends on the “treewidth” of the induced subgraph, where if the treewidth is small (as in trees) then the updates are efficient, and if the treewidth is large (as in fully-connected graphs) then these do not provide an advantage. Treewidth is related to the notion of “chordal” graphs (trees are special cases of chordal graphs) and chordal embeddings which have been exploited for matrix problems like covariance estimation [Dahl et al., 2008] and semidefinite programming [Sun et al., 2014, Vandenberghe and Andersen, 2015]. Considering “treewidth 2” or “treewidth 3” blocks would give more progress than our tree-based updates, although it is NP-hard to compute the treewidth of a general graph (but it is easy to upper-bound this quantity by simply choosing a random elimination order).

As opposed to structural constraints like requiring the graph to be a tree, it is now known that message-passing algorithms can solve linear systems with other properties like diagonal dominance or “attractive” coefficients [Malioutov et al., 2006]. There also exist specialized linear-time solvers for Laplacian matrices [Kyng and Sachdeva, 2016], and it would be interesting to explore BCD methods based on these structures. It would also be interesting to explore whether approximate message-passing algorithms which allow general graphs [Malioutov et al., 2006] can be used to improve optimization algorithms.

A Cost of Multi-Class Logistic Regression

The typical setting where we expect coordinate descent to outperform gradient descent is when the cost of one gradient descent iteration is similar to the cost of updating all variables via coordinate descent. It is well known that for the binary logistic regression objective, one of the most ubiquitous models in machine learning, coordinate descent with uniform random selection satisfies this property. We previously showed that this property is also satisfied for the GS rule in the case of logistic regression, provided that the data is sufficiently sparse [Nutini et al., 2015].

In this section we consider *multi-class* logistic regression. We first analyze the cost of gradient descent on this objective and how randomized coordinate descent is efficient for any sparsity level. Then we show that a high sparsity level is not sufficient for the GS rule to be efficient for this problem, but that it is efficient if we use a particular set of fixed blocks.

A.1 Cost of Gradient Descent

The likelihood for a single training example i with features $a_i \in \mathbb{R}^d$ and a label $b_i \in \{1, 2, \dots, k\}$ is given by

$$p(b_i|a_i, X) = \frac{\exp(x_{b_i}^T a_i)}{\sum_{c=1}^k \exp(x_c^T a_i)},$$

where x_c is column c of our matrix of parameters $X \in \mathbb{R}^{d \times k}$ (so the number of parameters n is dk). To maximize the likelihood over m independent and identically-distributed training examples we minimize the negative log-likelihood,

$$f(X) = \sum_{i=1}^m \left[-x_{b_i}^T a_i + \log \left(\sum_{c=1}^k \exp(x_c^T a_i) \right) \right], \quad (38)$$

which is a convex function. The partial derivative of this objective with respect to a particular X_{jc} is given by

$$\frac{\partial}{\partial X_{jc}} f(X) = - \sum_{i=1}^m a_{ij} \left[I(b_i = c) - \frac{\exp(x_c^T a_i)}{\sum_{c'=1}^k \exp(x_{c'}^T a_i)} \right], \quad (39)$$

where I is a 0/1 indicator variable and a_{ij} is feature j for training example i . We use A to denote a matrix where row i is given by a_i^T . To compute the full gradient, the operations which depend on the size of the problem are:

1. Computing $x_c^T a_i$ for all values of i and c .
2. Computing the sums $\sum_{c=1}^k \exp(x_c^T a_i)$ for all values of i .
3. Computing the partial derivative sums (39) for all values of j and c .

The first step is the result of the matrix multiplication AX , so if A has z non-zeroes then this has a cost of $O(zk)$ if we compute it using k matrix-vector multiplications. The second step costs $O(mk)$, which under the reasonable assumption that $m \leq z$ (since each row usually has at least one non-zero) is also in $O(zk)$. The third step is the result of a matrix multiplication of the form $A^T R$ for a (dense) m times k matrix R (whose elements have a constant-time cost to compute given the results of the first two steps), which also costs $O(zk)$ giving a final cost of $O(zk)$.

A.2 Cost of Randomized Coordinate Descent

Since there are $n = dk$ variables, we want our coordinate descent iterations to be dk -times faster than the gradient descent cost of $O(zk)$. Thus, we want to be able to implement coordinate descent iterations for a cost of $O(z/d)$ (noting that we always expect $z \geq d$ since otherwise we could remove some columns of A that only have zeroes). The key to doing this for randomized coordinate descent is to track two quantities:

1. The values $x_c^T a_i$ for all i and c .
2. The values $\sum_{c'=1}^k \exp(x_{c'}^T a_i)$ for all i .

Given these values we can compute the partial derivative in $O(z/d)$ in expectation, because this is the expected number of non-zero values of a_{ij} in the partial derivative sum (39) (A has z total non-zeroes and we are randomly choosing one of the d columns). Further, after updating a particular X_{jc} we can update the above quantities for the same cost:

1. We need to update $x_c^T a_i$ for the particular c we chose for the examples i where a_{ij} is non-zero for the chosen value of j . This requires an $O(1)$ operation (subtract the old $x_{jc} a_{ij}$ and add the new value) for each non-zero element of column j of A . Since A has z non-zeroes and d columns, the expected number of non-zeroes is z/d so this has a cost of $O(z/d)$.
2. We need to update $\sum_{c'=1}^k \exp(x_{c'}^T a_i)$ for all i where a_{ij} is non-zero for our chosen j . Since we expect z/d non-zero values of a_{ij} , the cost of this step is also $O(z/d)$.

Note that BCD is also efficient since if we update τ elements, the cost is $O(z\tau/d)$ by just applying the above logic τ times. In fact, step 2 and computing the final partial derivative has some redundant computation if we update multiple X_{jc} with the same c , so we might have a small performance gain in the block case.

A.3 Cost of Greedy Coordinate Descent (Arbitrary Blocks)

The cost of greedy coordinate descent is typically higher than randomized coordinate descent since we need to track *all* partial derivatives. However, consider the case where each row has at most z_r non-zeroes and each column has at most z_c non-zeroes. In this setting we previously showed that for binary logistic regression it is possible to track all partial derivatives for a cost of $O(z_r z_c)$, and that we can track the maximum gradient value at the cost of an additional logarithmic factor [Nutini et al., 2015, Appendix A].¹⁷ Thus, greedy coordinate selection has a similar cost to uniform selection when the sparsity pattern makes $z_r z_c$ similar to z/d (as in the case of a grid-structured dependency graph like Figure 3).

Unfortunately, having $z_r z_c$ similar to z/d is not sufficient in the multi-class case. In particular, the cost of tracking all the partial derivatives after updating an X_{jc} in the multi-class case can be broken down as follows:

1. We need to update $x_c^T a_i$ for the examples i where a_{ij} is non-zero. Since there are at most z_c non-zero values of a_{ij} over all i the cost of this is $O(z_c)$.
2. We need to update $\sum_{c'=1}^k \exp(x_{c'}^T a_i)$ for all i where a_{ij} is non-zero. Since there are at most z_c non-zero values of a_{ij} the cost of this is $O(z_c)$.
3. We need to update the partial derivatives $\partial f / \partial X_{jc}$ for all j and c . Observe that each time we have a_{ij} non-zero, we change the partial derivative with respect to all features j' that are non-zero in the example i and we must update all classes c' for these examples. Thus, for the $O(z_c)$ examples with a non-zero feature j we need to update up to $O(z_r)$ other features for that example and for each of these we need to update all k classes. This gives a cost of $O(z_r z_c k)$.

¹⁷Note that the purpose of the quantity $z_r z_c$ is to serve as a potentially-crude upper bound on the maximum degree in the dependency graph we describe in Section 5. Any tighter bound on this degree would yield a tighter upper bound on the runtime.

So while in the binary case we needed $O(z_r z_c)$ to be comparable to $O(z/d)$ for greedy coordinate descent to be efficient, in the multi-class case we now need $O(z_r z_c k)$ to be comparable to $O(z/d)$ in the multi-class case. This means that not only do we need a high degree of sparsity but we also need the number of classes k to be small for greedy coordinate descent to be efficient.

A.4 Cost of Greedy Coordinate Descent (Fixed Blocks)

Greedy rules are more expensive in the multi-class case because whenever we change an individual variable X_{jc} , it changes the partial derivative with respect to $X_{j'c'}$ for a set of j' values and for *all* c' . But we can improve the efficiency of greedy rules by using a special choice of fixed blocks that reduces the number of j' values. In particular, BCD is more efficient for the multi-class case if we put $X_{j'c'}$ for all c' into the same block. In other words, we ensure that each row of X is part of the same block so that we apply BCD to rows rather than in an unstructured way. Below we consider the cost of updating the needed quantities after changing an entire row of X_{jc} values:

1. Since we are updating k elements, the cost of updating the $x_c^T a_i$ is k -times larger giving $O(z_c k)$ when we update a row.
2. Similarly, the cost of updating the sums $\sum_{c=1}^k \exp(x_c^T a_i)$ is k -times larger also giving $O(z_c k)$.
3. Where we gain in computation is the cost of computing the changed values of the partial derivatives $\partial f / \partial X_{jc}$. As before, each time we have a_{ij} non-zero for our particular row j , we change the partial derivative with respect to all other j' for this example and with respect to each class c' for these j' . Thus, for the $O(z_c)$ examples with a non-zero feature j we need to update up to $O(z_r)$ other features for that example and for each of these we need to update all k classes. But since j is the same for each variable we update, we only have to do this once which gives us a cost of $O(z_r z_c k)$.

So the cost to update a row of the matrix X is $O(z_r z_c k)$, which is the same cost as only updating a single element. Considering the case of updating individual rows, this gives us d blocks so in order for BCD to be efficient it must be d -times faster than the gradient descent cost of $O(zk)$. Thus, we need a cost of $O(zk/d)$ per iteration. This is achieved if $O(z_r z_c)$ to be similar to $O(z/d)$, which is the same condition we needed in the binary case.

B Blockwise Lipschitz Constants

In this section we show how to derive lower-bounds on the block-Lipschitz constants of the gradient and Hessian for several common problem settings. We will use that a twice-differentiable function has an L -Lipschitz continuous gradient if and only if the absolute eigenvalues of its Hessian are upper-bounded by L ,

$$\|\nabla f(x) - \nabla f(y)\| \leq L\|x - y\| \iff \nabla^2 f(x) \preceq LI.$$

This implies that when considering blockwise constants we have

$$\|\nabla_b f(x + U_b d) - \nabla_b f(x)\| \iff \nabla_{bb}^2 f(x) \preceq L_b I.$$

Thus, bounding the blockwise eigenvalues of the Hessian bounds the blockwise Lipschitz constants of the gradient. We also use that this equivalence extends to the case of general quadratic norms,

$$\|\nabla_b f(x + U_b d) - \nabla_b f(x)\|_{H_b^{-1}} \leq \|d\|_{H_b} \iff \nabla_{bb}^2 f(x) \preceq H_b.$$

B.1 Quadratic Functions

Quadratic functions have the form

$$f(x) = \frac{1}{2}x^T A x + c^T x,$$

for a positive semi-definite matrix A and vector c . For all x the Hessian with respect to block b is given by the sub-matrix of A ,

$$\nabla_{bb}^2 f(x) = A_{bb}.$$

Thus, we have that L_b is given by the maximum eigenvalue of the submatrix, $L_b = \|A_b\|$ (the operator norm of the submatrix). In the special case where b only contains a single element i , we have that L_i is given by the absolute value of the diagonal element, $L_i = |A_{ii}|$. If we want to use a general quadratic norm we can simply take $H_b = A_{bb}$, which is cheaper to compute than the L_b (since it does not require an eigenvalue calculation).

B.2 Least Squares

The least squares objective has the form

$$f(x) = \frac{1}{2}\|Ax - c\|^2,$$

for a matrix A and vector c . This is a special case of a quadratic function, where the Hessian is given by

$$\nabla^2 f(x) = A^T A.$$

This gives us that $L_b = \|A_b\|^2$ (where A_b is the matrix containing the columns b of A). In the special case where the block has a single element j , observe that $L_j = \sum_{i=1}^m a_{ij}^2$ (sum of the squared values in column j) so we do not need to solve an eigenvalue problem. When using a quadratic norm we can take $H_b = A_b^T A_b$ which similarly does not require solving an eigenvalue problem.

B.3 Logistic Regression

The likelihood of a single example in a logistic regression model is given by

$$p(b_i|a_i, x) = \frac{1}{1 + \exp(-b_i x^T a_i)},$$

where each $a_i \in \mathbb{R}^d$ and $b_i \in \{-1, 1\}$. To maximize the likelihood over m examples (sampled independently) we minimize the negative log-likelihood,

$$f(x) = \sum_{i=1}^m \log(1 + \exp(-b_i x^T a_i)).$$

Using A as a matrix where row i is given by a_i^T and defining $h_i(x) = p(b_i|a_i, x)$, we have that

$$\begin{aligned} \nabla^2 f(x) &= \sum_{i=1}^m h_i(x)(1 - h_i(x))a_i a_i^T \\ &\leq 0.25 \sum_{i=1}^m a_i a_i^T \\ &= 0.25 A^T A. \end{aligned}$$

The generalized inequality above is the binary version of the Böhning bound [Böhning, 1992]. This bound can be derived by observing that $h_i(x)$ is in the range $(0, 1)$, so the quantity $h_i(x)(1 - h_i(x))$ has an upper bound of 0.25. This result means that we can use $L_b = 0.25\|A_b\|^2$ for block b , $L_j = 0.25 \sum_{i=1}^m a_{ij}^2$ for single-coordinate blocks, and $H_b = 0.25 A_b^T A_b$ if we are using a general quadratic norm (notice that computing H_b is again cheaper than computing L_b).

B.4 Multi-Class Logistic Regression

The Hessian of the multi-class logistic regression objective (38) with respect to parameter vectors x_c and $x_{c'}$ can be written as

$$\frac{\partial^2}{\partial x_c \partial x_{c'}} f(X) = \sum_{i=1}^m h_{i,c}(X)(I(c=c') - h_{i,c'}(X))a_i a_i^T,$$

where similar to the binary logistic regression case we have defined $h_{i,c} = p(c|a_i, X)$. This gives the full Hessian the form

$$\nabla^2 f(X) = \sum_{i=1}^m H_i(X) \otimes a_i a_i^T,$$

where we used \otimes to denote the Kronecker product and where element (c, c') of the k by k matrix $H_i(X)$ is given by $h_{i,c}(X)(I(c=c') - h_{i,c'}(X))$. Böhning's bound [Böhning, 1992] on this matrix is that

$$H_i(X) \preceq \frac{1}{2} \left(I - \frac{1}{k} \mathbf{1}\mathbf{1}^T \right),$$

where $\mathbf{1}$ is a vector of ones while recall that k is the number of classes. Using this we have

$$\begin{aligned} \nabla^2 f(X) &\preceq \sum_{i=1}^m \frac{1}{2} \left(I - \frac{1}{k} \mathbf{1}\mathbf{1}^T \right) \otimes a_i a_i^T \\ &= \frac{1}{2} \left(I - \frac{1}{k} \mathbf{1}\mathbf{1}^T \right) \otimes \sum_{i=1}^m a_i a_i^T \\ &= \frac{1}{2} \left(I - \frac{1}{k} \mathbf{1}\mathbf{1}^T \right) \otimes A^T A. \end{aligned}$$

As before we can take submatrices of this expression as our H_b , and we can take eigenvalues of the submatrices as our L_b . However, due to the $1/k$ factor we can actually obtain tighter bounds for sub-matrices of the Hessian that do not involve at least two of the classes. In particular, consider a sub-Hessian involving the variables only associated with k' classes for $k' < k$. In this case we can replace the k by k matrix $(I - (1/k)\mathbf{1}\mathbf{1}^T)$ with the k' by k' matrix $(I - (1/(k'+1))\mathbf{1}\mathbf{1}^T)$. The “+1” added to k' in the second term effectively groups all the other classes (whose variables are fixed) into a single class (the “+1” is included in Böhning's original paper as he fixes $x_k = 0$ and defines k to be one smaller than the number of classes). This means (for example) that we can take $L_j = 0.25 \sum_{i=1}^m a_{ij}^2$ as in the binary case rather than the slightly-larger diagonal element $0.5(1 - 1/k) \sum_{i=1}^m a_{ij}^2$ in the matrix above.¹⁸

C Derivation of GSD Rule

In this section we derive a progress bound for twice-differentiable convex functions when we choose and update the block b_k according to the GSD rule with $D_{b,i} = L_i \tau$ (where τ is the maximum block size). We start by using the Taylor series representation of $f(x^{k+1})$ in terms of $f(x^k)$ and some z between x^{k+1} and

¹⁸The binary logistic regression case can conceptually be viewed as a variation on the softmax loss where we fix $x_c = 0$ for one of the classes and thus are always only updating variables from class. This gives the special case of $0.5(I - 1/(k+1)\mathbf{1}\mathbf{1}^T)A^T A = 0.5(1 - 0.5)A^T A = 0.25A^T A$, the binary logistic regression bound from the previous section.

x^k (keeping in mind that these only differ along coordinates in b_k),

$$\begin{aligned}
f(x^{k+1}) &= f(x^k) + \langle \nabla f(x^k), x^{k+1} - x^k \rangle + \frac{1}{2}(x^{k+1} - x^k)^T \nabla_{b_k b_k}^2 f(z)(x^{k+1} - x^k) \\
&\leq f(x^k) + \langle \nabla f(x^k), x^{k+1} - x^k \rangle + \frac{|b_k|}{2} \sum_{i \in b_k} \nabla_{ii}^2 f(z)(x_i^{k+1} - x_i^k)^2 \\
&\leq f(x^k) + \langle \nabla f(x^k), x^{k+1} - x^k \rangle + \frac{\tau}{2} \sum_{i \in b_k} \nabla_{ii}^2 f(z)(x_i^{k+1} - x_i^k)^2 \\
&\leq f(x^k) + \langle \nabla f(x^k), x^{k+1} - x^k \rangle + \frac{\tau}{2} \sum_{i \in b_k} L_i (x_i^{k+1} - x_i^k)^2,
\end{aligned}$$

where the first inequality follows from convexity of f which implies that $\nabla_{b_k b_k}^2 f(x^k)$ is positive semi-definite and by Lemma 1 of Nesterov's coordinate descent paper [Nesterov, 2010]. The second inequality follows from the definition of τ and the third follows from the definition of L_i . Now using our choice of $D_{b,i} = L_i \tau$ in the update we have for $i \in b_k$ that

$$x_i^{k+1} = x_i^k - \frac{1}{L_i \tau} \nabla_i f(x^k),$$

which yields

$$\begin{aligned}
f(x^{k+1}) &\leq f(x^k) - \frac{1}{2\tau} \sum_{i \in b_k} \frac{|\nabla_i f(x^k)|^2}{L_i} \\
&= f(x^k) - \frac{1}{2} \max_b \sum_{i \in b} \frac{|\nabla_i f(x^k)|^2}{L_i \tau} \\
&= f(x^k) - \|\nabla f(x^k)\|_{\mathcal{B}}^2.
\end{aligned}$$

The first equality uses that we are selecting b_k using the GSD rule with $D_{b,i} = L_i \tau$ and the second inequality follows from the definition of the mixed norm $\|\cdot\|_{\mathcal{B}}$ from Section 3.5 with $H_b = D_b$. This progress bound implies that the convergence rate results in that section also hold.

D Efficiently Testing the Forest Property

In this section we give a method to test whether adding a node to an existing forest maintains the forest property. In this setting our input is an undirected graph G and a set of nodes b whose induced subgraph G_b forms a forest (has no cycles). Given a node i , we want to test whether adding i to b will maintain that the induced subgraph is acyclic. In this section we show how to do this in $O(p)$, where p is the degree of the node i .

The method is based on the following simple observations:

- If the new node i introduces a cycle, then it must be part of the cycle. This follows because G_b is assumed to be acyclic, so no cycles can exist that do not involve i .
- If i introduces a cycle, we can arbitrarily choose i to be the start and end point of the cycle.
- If the new node i has 1 or fewer neighbours in b , then it does not introduce a cycle. With no neighbours it clearly can not be part of a cycle. With one neighbour, we would have to traverse its one edge more than once to have it start and end a path.
- If the new node i has at least 2 neighbours in b that are part of the same tree, then i introduces a cycle. Specifically, we can construct a cycle as follows: we start at node i , go to one of its neighbours, follow a path through the tree to another one of its neighbours in the same tree (such a path exists because trees are connected by definition), and then return to node i .

- If the new node i has at least 2 neighbours in b but they are all in different trees, then i does not introduce a cycle. This is similar to the case where i has only one edge: any path that starts and ends at node i would have to traverse one of its edges more than once (because the disjoint trees are not connected to each other).

The above cases suggest that to determine whether adding node i to the forest b maintains the forest property, we only need to test whether node i is connected to two nodes that are part of the same tree in the existing forest. We can do this in $O(p)$ using the following data structures:

1. For each of the n nodes, a list of the adjacent nodes in G .
2. A set of n labels in $\{0, 1, 2, \dots, t\}$, where t is the number of trees in the existing forest. This number is set to 0 for nodes that are not in b , is set to 1 for nodes in the first tree, is set to 2 for nodes in the second tree, and so on.

Note that there is no ordering to the labels $\{1, 2, \dots, t\}$, each tree is just assigned an arbitrary number that we will use to determine if nodes are in the same tree. We can find all neighbours of node i in $O(p)$ using the adjacency list, and we can count the number of neighbours in each tree in $O(p)$ using the tree numbers. If this count is at least 2 for any tree then the node introduces a cycle, and otherwise it does not.

In the algorithms of Section 5.1 and 5.2, we also need to update the data structures after adding a node i to b that maintains the forest property. For this update we need to consider three scenarios:

- If the node i has one neighbour in b , we assign it the label of its neighbour.
- If the node i has no neighbours in b , we assign it the label $(t + 1)$ since it forms a new tree.
- If the node i has multiple neighbours in b , we need to merge all the trees it is connected to.

The first two steps cost $O(1)$, but a naive implementation of the third step would cost $O(n)$ since we could need to re-label almost all of the nodes. Fortunately, we can reduce the cost of this merge step to $O(p)$. This requires a relaxation of the condition that the labels represent disjoint trees. Instead, we only require that nodes with the same label are part of the same tree. This allows multiple labels to be associated with each tree, but using an extra data structure we can still determine if two labels are part of the same tree:

3. A list of t numbers, where element j gives the *minimum node number* in the tree that j is part of.

Thus, given the labels of two nodes we can determine whether they are part of the same tree in $O(1)$ by checking whether their minimum node numbers agree. Given this data structure, the merge step is simple: we arbitrarily assign the new node i to the tree of one of its neighbours, we find the minimum node number among the p trees that need to be merged, and then we use this as the minimum node number for all p trees. This reduces the cost to $O(p)$.

Given that we can efficiently test the forest property in $O(p)$ for a node with p neighbours, it follows that the total cost of the greedy algorithm from Section 5.2 is $O(n \log n + |E|)$ given the gradient vector and adjacency lists. The $O(n \log n)$ factor comes from sorting the gradient values, and the number of edges $|E|$ is 2 times the sum of the p values. If this cost is prohibitive, one could simply restrict the number of nodes that we consider adding to the forest to reduce this time.

E Functions Bound Iterates under Strong-Convexity

Defining $F(x)$ as $F(x) = f(x) + g(x)$ in the “smooth plus separable non-smooth” setting of (27), existing works on cyclic [Beck and Tetruashvili, 2013] and greedy selection [Nutini et al., 2015] of i_k within proximal coordinate descent methods imply that

$$F(x^k) - F(x^*) \leq \rho^k [F(x^0) - F(x^*)], \quad (40)$$

for some $\rho < 1$ when f is strongly-convex. Note that strong-convexity of f implies strong-convexity of F , so we have that

$$F(y) \geq F(x) + \langle s, y - x \rangle + \frac{\mu}{2} \|y - x\|^2,$$

where μ is the strong-convexity constant of f and s is any subgradient of F at x . Taking $y = x^k$ and $x = x^*$ we obtain that

$$F(x^k) \geq F(x^*) + \frac{\mu}{2} \|x^k - x^*\|^2, \quad (41)$$

which uses that 0 is in the sub-differential of F at x^* . Thus we have that

$$\|x^k - x^*\|^2 \leq \frac{2}{\mu} [F(x^k) - F(x^*)] \leq \frac{2}{\mu} \rho^k [F(x^0) - F(x^*)],$$

which is the type of convergence rate we assume in Section 6.2 with $\gamma = \frac{2}{\mu} [F(x^0) - F(x^*)]$.

F Full Experimental Results

In this section we first provide details on the datasets, and then we present our complete set of experimental results.

F.1 Datasets

We considered these five datasets:

- A A least squares problem with a data matrix $A \in \mathbb{R}^{m \times n}$ and target $b \in \mathbb{R}^m$,

$$\arg \min_{x \in \mathbb{R}^n} \frac{1}{2} \|Ax - b\|^2.$$

We set A to be an m by n matrix with entries sampled from a $\mathcal{N}(0, 1)$ distribution (with $m = 1000$ and $n = 10000$). We then added 1 to each entry (to induce a dependency between columns), multiplied each column by a sample from $\mathcal{N}(0, 1)$ multiplied by ten (to induce different Lipschitz constants across the coordinates), and only kept each entry of A non-zero with probability $10 \log(m)/m$. We set $b = Ax + e$, where the entries of e were drawn from a $\mathcal{N}(0, 1)$ distribution while we set 90% of x to zero and drew the remaining values from a $\mathcal{N}(0, 1)$ distribution.

- B A binary logistic regression problem of the form

$$\arg \min_{x \in \mathbb{R}^n} \sum_{i=1}^n \log(1 + \exp(-b_i x^T a_i)).$$

We use the data matrix A from the previous dataset (setting row i of A to a_i^T), and b_i to be the sign of $x^T a_i$ using the x used in the generating the previous dataset. We then flip the sign of each entry in b with probability 0.1 to make the dataset non-separable.

- C A multi-class logistic regression problem of the form

$$\arg \min_{x \in \mathbb{R}^{d \times k}} \sum_{i=1}^m \left[-x_{b_i}^T a_i + \log \left(\sum_{c=1}^k \exp(x_c^T a_i) \right) \right],$$

see (38). We generate a 1000 by 1000 matrix A as in the previous two cases. To generate the $b_i \in \{1, 2, \dots, k\}$ (with $k = 50$), we compute $AX + E$ where the elements of the matrices $X \in \mathbb{R}^{d \times k}$ and $E \in \mathbb{R}^{m \times k}$ are sampled from a standard normal distribution. We then compute the maximum index in each row of that matrix as the class labels.

D A label propagation problem of the form

$$\min_{x_i \in S'} \frac{1}{2} \sum_{i=1}^n \sum_{j=1}^n w_{ij} (x_i - x_j)^2,$$

where x is our label vector, S is the set of labels that we do know (these x_i are set to a sample from a normal distribution with a variance of 100), S' is the set of labels that we do not know, and $w_{ij} \geq 0$ are the weights assigned to each x_i describing how strongly we want the labels x_i and x_j to be similar. We set the non-zero pattern of the w_{ij} so that the graph forms a 50 by 50 lattice-structure (setting the non-zero values to 10000). We labeled 100 points, leading to a problem with 2400 variables but where each variable has at most 4 neighbours in the graph.

E Another label propagation problem for semi-supervised learning in the ‘two moons’ dataset [Zhou et al., 2003], which is binary label propagation problem ($x_i \in [-1, 1]$). We generate 2000 samples from this dataset, randomly label 100 points in the data, and connect each node to its five nearest neighbours (using $w_{ij} = 1$). This results in a very sparse but unstructured graph.

F.2 Greedy Rules with Gradients Updates

In Figure 8 we show the performance of the different methods from Section 7.1 on all five datasets with three different block sizes. In Figure 9 we repeat the experiment but focusing only on the FB methods. For each FB method, we plot the performance using our upper bounds on L_b as the step-size (Lb) and using the Lipschitz approximation procedure from Section 4.3 (LA). Here we see the LA methods improves performance when using large block sizes and in cases where the global L_b bound is not tight.

Our third experiment also focused on the FB methods, but considered different ways to partition the variables into fixed blocks. We considered three approaches:

1. Order: we partition the variables based on their numerical order (which is similar to using a random order for dataset except Dataset D, where this method groups variables that adjacent in the lattice).
2. Avg: we compute the coordinate-wise Lipschitz constants L_i , and place the largest L_i with the smallest L_i values so that the average L_i values are similar across the blocks.
3. Sort: we sort the L_i values and place the largest values together (and the smallest values together).

We compared many variations on cyclic/random/greedy rules with gradient or matrix updates. In the case of greedy rules with gradient updates, we found that the Sort method tended to perform the best while the Order method tended to perform the worst (see Figure 10). When using matrix updates or when using cyclic/randomized rules, we found that no partitioning strategy dominated other strategies.

F.3 Greedy Rules with Matrix and Newton Updates

In Figure 11 we show the performance of the different methods from Section 7.2 on all five datasets with three different block sizes. In Figure 12 we repeat this experiment on the two non-quadratic problems, using the Newton direction and a line-search rather than matrix updates. We see that using Newton’s method significantly improves performance over matrix updates.

F.4 Proximal Updates using Random Selection

In Figure 7 we compare the performance of a projected gradient update with L_b step-size, a projected Newton (PN) solver with line search and the two-metric projection (TMP) update when using greedy selected fixed (FB) and variable (VB) blocks of different sizes ($|b| = 5, 50, 100$). In Figure 13 we repeat this experiment using randomly selected blocks. We see that for such a sparse problem the random block selection rules suffer from selecting variables that are already zero/active, as seen by the step-like nature of the results.

Acknowledgments

We would like to thank Dr. Warren Hare for fruitful conversations that helped with Section 6. We would also like to thank Francis Bach, Coralia Cartis, Aleksandar Dogandzic, Ives Macedo, Anastasia Podosinnikova, and Suvrit Sra for valuable discussions. This work was supported by a Discovery Grant from the Natural Sciences and Engineering Research Council of Canada (NSERC). Julie Nutini and Issam Laradji are funded by UBC Four-Year Doctoral Fellowships (4YFs).

References

- S. Bakin. *Adaptive regression and model selection in data mining problems*. PhD thesis, Australian National University, Canberra, Australia, 1999.
- A. Beck and L. Tetruashvili. On the convergence of block coordinate descent type methods. *SIAM J. Optim.*, 23(4):2037–2060, 2013.
- D. P. Bertsekas. On the Goldstein-Levitin-Polyak gradient projection method. *IEEE Transactions on Automatic Control*, 21(2):174–184, 1976.
- D. P. Bertsekas. *Nonlinear Programming*. Athena Scientific, 3rd edition, 2016.
- D. Bickson. *Gaussian Belief Propagation: Theory and Application*. PhD thesis, The Hebrew University of Jerusalem, Jerusalem, Israel, 2009.
- T. Blumensath and M. E. Davies. Iterative hard thresholding for compressed sensing. *Appl. Comput. Harmon. Anal.*, 27(3):265–274, 2009.
- L. Bo and C. Sminchisescu. Greedy block coordinate descent for large scale Gaussian process regression. *arXiv:1206.3238*, 2012.
- D. Böhning. Multinomial logistic regression algorithm. *Ann. Inst. Stat. Math.*, 44(1):197–200, 1992.
- S. Boyd and L. Vandenberghe. *Convex Optimization*. Cambridge University Press, 2004.
- J. V. Burke and J. J. Moré. On the identification of active constraints. *SIAM J. Numer. Anal.*, 25(5):1197–1211, 1988.
- C.-C. Chang and C.-J. Lin. LIBSVM: A library for support vector machines. *ACM Trans. Intell. Syst. Technol.*, 2(3):27:1–27:27, 2011. Software available at <http://www.csie.ntu.edu.tw/~cjlin/libsvm>.
- B. Chen, S. He, Z. Li, and S. Zhang. Maximum block improvement and polynomial optimization. *SIAM J. Optim.*, 22(1):87–107, 2012.
- D. Csiba and P. Richtárik. Importance sampling for minibatches. *arXiv:1602.02283*, 2016.
- D. Csiba and P. Richtárik. Global convergence of arbitrary-block gradient methods for generalized Polyak-Lojasiewicz functions. *arXiv:1709.03014*, 2017.
- D. Csiba, Z. Qu, and P. Richtárik. Stochastic dual coordinate ascent with adaptive probabilities. In *Proceedings of the 32nd International Conference on Machine Learning*, pages 674–683, Lille, France, 2015.
- J. Dahl, L. Vandenberghe, and V. Roychowdhury. Covariance selection for nonchordal graphs via chordal embedding. *Optim. Methods Softw.*, 23(4):501–520, 2008.

- M. De Santis, S. Lucidi, and F. Rinaldi. A fast active set block coordinate descent algorithm for ℓ_1 -regularized least squares. *SIAM J. Optim.*, 26(1):781–809, 2016.
- R. S. Dembo, S. C. Eisenstat, and T. Steihaug. Inexact Newton methods. *SIAM J. Numer. Anal.*, 19(2):400–408, 1982.
- J. E. Dennis and J. J. Moré. A characterization of superlinear convergence and its application to quasi-Newton methods. *Math. Comput.*, 28(126):549–560, 1974.
- I. S. Dhillon, P. K. Ravikumar, and A. Tewari. Nearest neighbor based greedy coordinate descent. In *Advances in Neural Information Processing Systems 24*, pages 2160–2168, 2011.
- B. Efron, T. Hastie, I. Johnstone, and R. Tibshirani. Least angle regression. *Ann. Stat.*, 32(2):407–451, 2004.
- A. Ene and H. L. Nguyen. Random coordinate descent methods for minimizing decomposable submodular functions. In *Proceedings of the 32nd International Conference on Machine Learning*, pages 787–795, Lille, France, 2015.
- L. Esperet, L. Lemoine, and F. Maffray. Equitable partition of graphs into induced forests. *Discrete Math.*, 338:1481–1483, 2015.
- O. Fercoq and P. Richtárik. Accelerated, parallel and proximal coordinate descent. *SIAM J. Optim.*, 25(4):1997–2023, 2015.
- K. Fountoulakis and R. Tappenden. A flexible coordinate descent method. *arXiv:1507.03713*, 2015.
- K. Fountoulakis, F. Roosta-Khorasani, J. Shun, X. Cheng, and M. W. Mahoney. Exploiting optimization for local graph clustering. *arXiv:1602.01886*, 2016.
- W. J. Fu. Penalized regressions: the bridge versus the lasso. *J. Comput. Graph. Stat.*, 7(3):397–416, 1998.
- E. M. Gafni and D. P. Bertsekas. Two-metric projection methods for constrained optimization. *SIAM J. Control Optim.*, 22(6):936–964, 1984.
- M. R. Garey and D. S. Johnson. *Computers and Intractability: A Guide to the Theory of NP-Completeness*. W. H. Freeman & Co., New York, NY, USA, 1979.
- T. Glasmachers and U. Dogan. Accelerated coordinate descent with adaptive coordinate frequencies. In *Proceedings of the 5th Asian Conference on Machine Learning*, pages 72–86, Canberra, Australia, 2013.
- J. Gregor and J. A. Fessler. Comparison of SIRT and SQS for regularized weighted least squares image reconstruction. *IEEE Trans. Comput. Imaging*, 1(1):44–55, 2015.
- W. L. Hare. Identifying active manifolds in regularization problems. In H. H. Bauschke, R. S. Burachik, P. L. Combettes, V. Elser, D. R. Luke, and H. Wolkowicz, editors, *Fixed-Point Algorithms for Inverse Problems in Science and Engineering*, pages 261–271. Springer New York, New York, NY, 2011.
- W. L. Hare and A. S. Lewis. Identifying active constraints via partial smoothness and prox-regularity. *J. Convex Analysis*, 11(2):251–266, 2004.
- T. Hastie, S. Rosset, R. Tibshirani, and J. Zhu. The entire regularization path for the support vector machine. *J. Mach. Learn. Res.*, 5:1391–1415, 2004.
- R. R. Hocking. A biometrics invited paper. The analysis and selection of variables in linear regression. *Biometrics*, 32(1):1–49, 1976.

- C.-J. Hsieh, M. A. Sustik, I. S. Dhillon, P. K. Ravikumar, and R. Poldrack. BIG & QUIC: Sparse inverse covariance estimation for a million variables. In *Advances in Neural Information Processing Systems 26*, pages 3165–3173, 2013.
- S. Jegelka, F. Bach, and S. Sra. Reflection methods for user-friendly submodular optimization. In *Advances in Neural Information Processing Systems 26*, pages 1313–1321, 2013.
- T. Joachims. Making large-scale SVM learning practical. In B. Schölkopf, C. J. C. Burges, and A. J. Smola, editors, *Advances in Kernel Methods - Support Vector Learning*, pages 169–184. MIT Press, 1999.
- H. Karimi, J. Nutini, and M. Schmidt. Linear convergence of gradient and proximal-gradient methods under the Polyak-Lojasiewicz condition. In *Machine Learning and Knowledge Discovery in Databases: European Conference, ECML PKDD 2016, Proceedings, Part I*, pages 795–811, Riva del Garda, Italy, 2016.
- M. E. Khan. *Variational Learning for Latent Gaussian Model of Discrete Data*. PhD thesis, The University of British Columbia, Vancouver, Canada, 2012.
- R. Kyng and S. Sachdeva. Approximate Gaussian elimination for Laplacians - fast, sparse, and simple. In *Foundations of Computer Science (FOCS), 2016 IEEE 57th Annual Symposium on*, pages 573–582. IEEE, 2016.
- C.-P. Lee and S. J. Wright. Random permutations fix a worst case for cyclic coordinate descent. *arXiv:1607.08320*, 2016.
- J. D. Lee, Y. Sun, and M. A. Saunders. Proximal Newton-type methods for convex optimization. In *Advances in Neural Information Processing Systems 25*, pages 827–835, 2012.
- S. Lee and S. J. Wright. Manifold identification in dual averaging for regularized stochastic online learning. *J. Mach. Learn. Res.*, 13(Jun):1705–1744, 2012.
- Q. Lei, K. Zhong, and I. S. Dhillon. Coordinate-wise power method. In *Advances in Neural Information Processing Systems 29*, pages 2064–2072, 2016.
- Z. Li, A. Uschmajew, and S. Zhang. On convergence of the maximum block improvement method. *SIAM J. Optim.*, 25(1):210–233, 2015.
- J. Mairal and B. Yu. Complexity analysis of the lasso regularization path. In *Proceedings of the 29th International Conference on Machine Learning*, pages 353–360, New York, NY, USA, 2012.
- D. M. Malioutov, J. K. Johnson, and A. S. Willsky. Walk-sums and belief propagation in Gaussian graphical models. *J. Mach. Learn. Res.*, 7(Oct):2031–2064, 2006.
- N. Megiddo. Combinatorial optimization with rational objective functions. *Math. Oper. Res.*, 4(4):414–424, 1979.
- L. Meier, S. Van De Geer, and P. Bühlmann. The group lasso for logistic regression. *J. R. Stat. Soc. Series B Stat. Methodol.*, 70(1):53–71, 2008.
- O. Meshi, T. Jaakkola, and A. Globerson. Convergence rate analysis of MAP coordinate minimization algorithms. In *Advances in Neural Information Processing Systems 25*, pages 3014–3022, 2012.
- R. Mifflin and C. Sagastizábal. Proximal points are on the fast track. *J. Convex Anal.*, 9(2):563–579, 2002.
- H. Namkoong, A. Sinha, S. Yadlowsky, and J. C. Duchi. Adaptive sampling probabilities for non-smooth optimization. In *Proceedings of the 34th International Conference on Machine Learning*, pages 2574–2583, Sydney, Australia, 2017.

- Y. Nesterov. *Introductory Lectures on Convex Optimization: A Basic Course*. Kluwer Academic Publishers, Dordrecht, The Netherlands, 2004.
- Y. Nesterov. Efficiency of coordinate descent methods on huge-scale optimization problems. *CORE Discussion Paper*, 2010.
- Y. Nesterov. Efficiency of coordinate descent methods on huge-scale optimization problems. *SIAM J. Optim.*, 22(2):341–362, 2012.
- Y. Nesterov and B. T. Polyak. Cubic regularization of Newton method and its global performance. *Math. Program.*, pages 177–205, 2006.
- J. Nocedal and S. J. Wright. *Numerical Optimization*. Springer, 1999.
- J. Nutini, M. Schmidt, I. H. Laradji, M. Friedlander, and H. Koepke. Coordinate descent converges faster with the Gauss-Southwell rule than random selection. In *Proceedings of the 32nd International Conference on Machine Learning*, pages 1632–1641, Lille, France, 2015.
- J. Nutini, M. Schmidt, and W. Hare. “Active-set complexity” of proximal gradient: How long does it take to find the sparsity pattern? *arXiv:1712.03577*, 2017.
- J. M. Ortega and W. C. Rheinboldt. *Iterative Solution of Nonlinear Equations in Several Variables*. New York: Academic Press, 1970.
- M. R. Osborne and B. A. Turlach. A homotopy algorithm for the quantile regression lasso and related piecewise linear problems. *J. Comput. Graph. Stat.*, 20(4):972–987, 2011.
- M. R. Osborne, B. Presnell, and B. A. Turlach. A new approach to variable selection in least squares problems. *IMA J. Numer. Anal.*, 20(3):389–403, 2000.
- S. Parter. The use of linear graphs in Gauss elimination. *SIAM Rev.*, 3(2):119–130, 1961.
- Y. C. Pati, R. Rezaifar, and P. S. Krishnaprasad. Orthogonal matching pursuit: Recursive function approximation with applications to wavelet decomposition. In *Proceedings of the 27th Annu. Asilomar Conf. Signals, Systems and Computers*, pages 40–44. IEEE, 1993.
- M. Pilanci and M. J. Wainwright. Newton sketch: A linear-time optimization algorithm with linear-quadratic convergence. *SIAM J. Optim.*, 27(1):205–245, 2017.
- J. C. Platt. Sequential minimal optimization: A fast algorithm for training support vector machines. Technical report, Microsoft Research, 1998.
- B. T. Polyak. Gradient methods for minimizing functionals (in Russian). *Zh. Vychisl. Mat. Mat. Fiz.*, pages 643–653, 1963.
- Z. Qin, K. Scheinberg, and D. Goldfarb. Efficient block-coordinate descent algorithms for Group Lasso. *Mathematical Programming Computation*, 5:143–169, 2013.
- Z. Qu and P. Richtárik. Coordinate descent with arbitrary sampling I: Algorithms and complexity. *Optim. Methods Softw.*, 31(5):829–857, 2016.
- Z. Qu and P. Richtárik. Coordinate descent with arbitrary sampling II: Expected separable overapproximation. *Optim. Methods Softw.*, 31(5):858–884, 2016.
- Z. Qu, P. Richtárik, and T. Zhang. Randomized dual coordinate ascent with arbitrary sampling. *arXiv:1411.5873*, 2014.

- Z. Qu, P. Richtárik, M. Takáč, and O. Fercoq. SDNA: Stochastic dual coordinate ascent for empirical risk minimization. In *Proceedings of the 33rd International Conference on Machine Learning*, pages 1823–1832, New York, New York, USA, 2016.
- P. Richtárik and M. Takáč. Parallel coordinate descent methods for big data optimization. *Math. Prog.*, 156(1-2):433–484, 2016.
- P. Richtárik and M. Takáč. Iteration complexity of randomized block-coordinate descent methods for minimizing a composite function. *Math. Program.*, 144:1–38, 2014.
- P. Richtárik and M. Takáč. On optimal probabilities in stochastic coordinate descent methods. *Optimization Letters*, 10(6):1233–1243, 2016.
- R. T. Rockafellar. Monotone operators and the proximal point algorithm. *SIAM J. Control Optim.*, 14(5):877898, 1976.
- D. J. Rose. Triangulated graphs and the elimination process. *J. Math. Anal. Appl.*, 32(3):597–609, 1970.
- S. Rosset and J. Zhu. Piecewise linear regularized solution paths. *Ann. Stat.*, 35(3):1012–1030, 2007.
- S. Sardy, A. G. Bruce, and P. Tseng. Block coordinate relaxation methods for nonparametric wavelet denoising. *J. Comput. Graph. Stat.*, 9(2):361–379, 2000.
- K. Scheinberg and I. Rish. SINCO—a greedy coordinate ascent method for sparse inverse covariance selection problem. *preprint*, 2009.
- C. Scherrer, A. Tewari, M. Halappanavar, and D. J. Haglin. Feature clustering for accelerating parallel coordinate descent. In *Advances in Neural Information Processing Systems 25*, pages 28–36, 2012.
- M. Schmidt. *Graphical Model Structure Learning with ℓ_1 -Regularization*. PhD thesis, The University of British Columbia, Vancouver, Canada, 2010.
- O. Shental, P. H. Siegel, J. K. Wolf, D. Bickson, and D. Dolev. Gaussian belief propagation solver for systems of linear equations. In *Information Theory, 2008. ISIT 2008. IEEE International Symposium on*, pages 1863–1867, Toronto, Canada, 2008. IEEE.
- A. Srinivasan and E. Todorov. Graphical Newton. *arXiv:1508.00952*, 2015.
- S. U. Stich, A. Raj, and M. Jaggi. Approximate steepest coordinate descent. *arXiv:1706.08427*, 2017.
- Y. Sun, M. S. Andersen, and L. Vandenberghe. Decomposition in conic optimization with partially separable structure. *SIAM J. Optim.*, 24(2):873–897, 2014.
- R. Tappenden, P. Richtárik, and J. Gondzio. Inexact coordinate descent: Complexity and preconditioning. *J. Optim. Theory Appl.*, pages 144–176, 2016.
- G. Thoppe, V. S. Borkar, and D. Garg. Greedy block coordinate descent (GBCD) method for high dimensional quadratic programs. *arXiv:1404.6635*, 2014.
- P. Tseng and S. Yun. A coordinate gradient descent method for nonsmooth separable minimization. *Math. Program.*, 117:387–423, 2009a.
- P. Tseng and S. Yun. Block-coordinate gradient descent method for linearly constrained nonsmooth separable optimization. *J. Optim. Theory Appl.*, pages 513–535, 2009b.
- L. Vandenberghe and M. S. Andersen. Chordal graphs and semidefinite optimization. *Found. Trends Optim.*, 1(4):241–433, 2015.

- D. J. Welsh and M. B. Powell. An upper bound for the chromatic number of a graph and its application to timetabling problems. *The Computer Journal*, 10(1):85–86, 1967.
- S. J. Wright. Identifiable surfaces in constrained optimization. *SIAM J. Control Optim.*, 31(4):1063–1079, 1993.
- S. J. Wright. Accelerated block-coordinate relaxation for regularized optimization. *SIAM J. Optim.*, 22(1):159–186, 2012.
- Y. Xu and W. Yin. A block coordinate descent method for regularized multiconvex optimization with applications to nonnegative tensor factorization and completion. *SIAM J. Imaging Sci*, 6(3):1758–1789, 2013.
- Y. You, X. Lian, J. Liu, H.-F. Yu, I. S. Dhillon, J. Demmel, and C.-J. Hsieh. Asynchronous parallel greedy coordinate descent. In *Advances in Neural Information Processing Systems 29*, pages 4682–4690, 2016.
- H.-F. Yu, C.-J. Hsieh, S. Si, and I. S. Dhillon. Scalable coordinate descent approaches to parallel matrix factorization for recommender systems. In *Data Mining (ICDM), 2012 IEEE 12th International Conference on*, pages 765–774. IEEE, 2012.
- D. Zhou, O. Bousquet, T. N. Lal, J. Weston, and B. Schölkopf. Learning with local and global consistency. In *Advances in Neural Information Processing Systems 16*, pages 321–328, 2003.

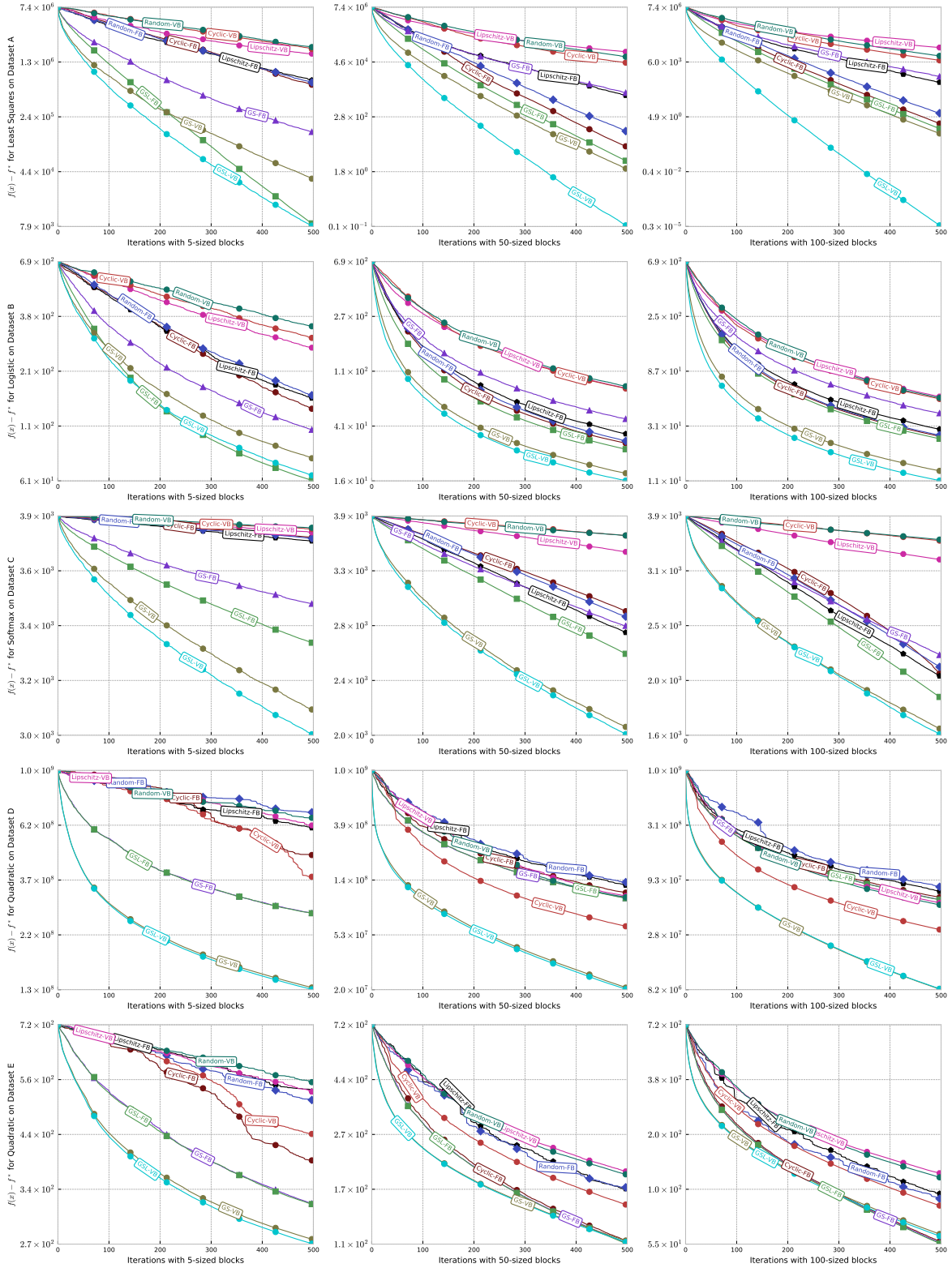


Figure 8: Comparison of different random and greedy block selection rules on five different problems (rows) with three different blocks (columns) when using gradient updates.

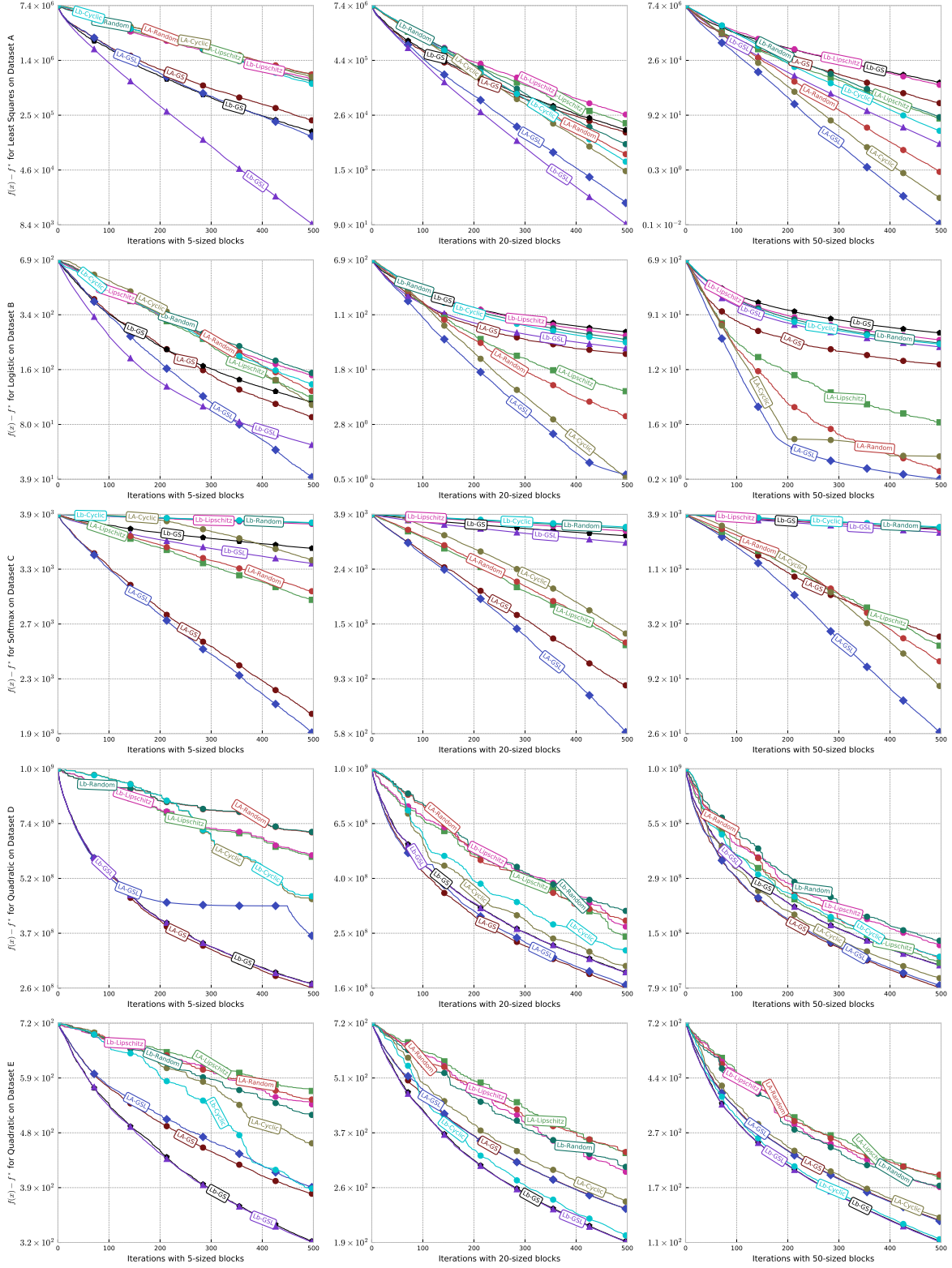


Figure 9: Comparison of different random and greedy block selection rules with gradient updates and fixed blocks, using two different strategies to estimate L_b .

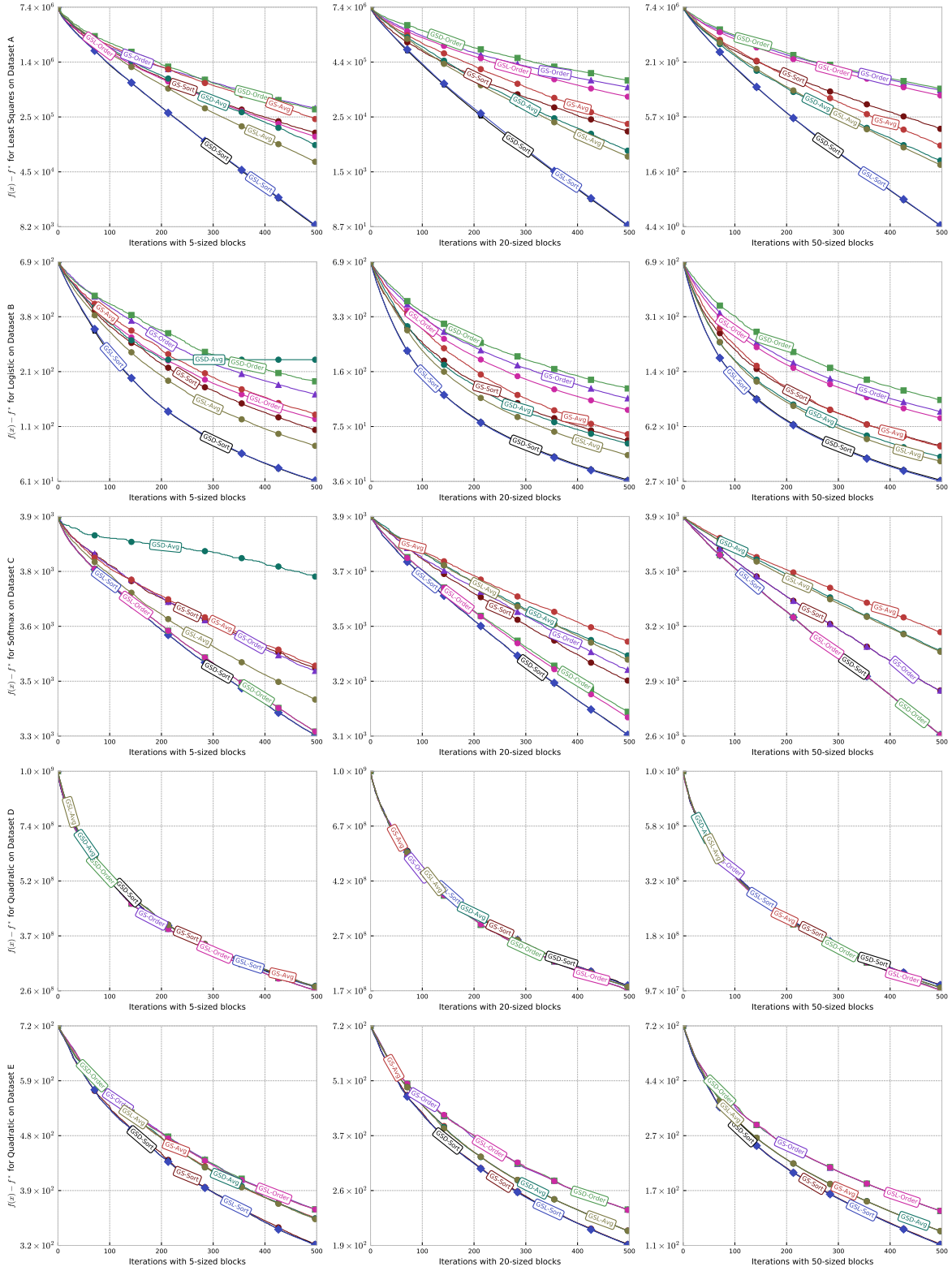


Figure 10: Comparison of different random and greedy block selection rules with gradient updates and fixed blocks, using three different ways to partition the variables into blocks.

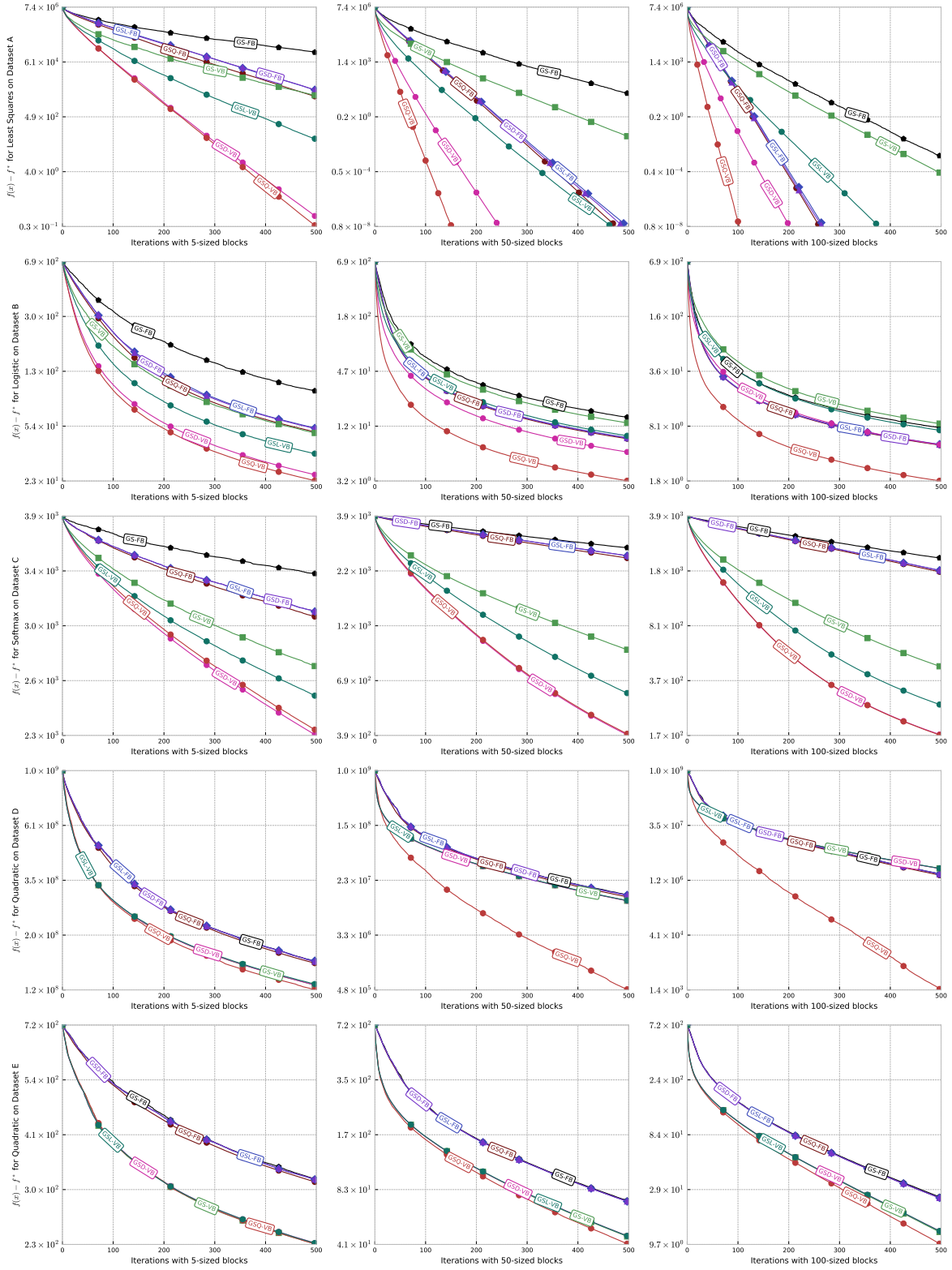


Figure 11: Comparison of different greedy block selection rules when using matrix updates.

